

AN ABSTRACT OF THE THESIS OF

Kuo-heng Lee for the Master of Science
(Name of student) (Degree)
in Oceanography presented on April 25, 1967
(Major) (Date)

Title: GEOPOTENTIAL ANOMALY AND GEOSTROPHIC FLOW OFF
NEWPORT, OREGON

Abstract approved: Redacted for Privacy
Dr. June G. Pattullo

The geopotential anomalies and the average meridional geostrophic flow off Newport, Oregon, were computed from the data taken during twenty-one hydrographic cruises.

The annual average of geopotential anomaly was 1.31 dynamic meters with a seasonal variation of the order of 14 dynamic centimeters. Highest values of geopotential anomaly occurred in September; lowest values occurred in April. Both the highest and lowest value of geopotential anomaly occurred at 105 nautical miles offshore.

The currents found by dynamic computation were weak and irregular, generally 5 cm/sec or less. The direction of the average meridional geostrophic flow varied with season. Within 105 nautical miles of the coast, flow was southward in summer, northward in winter. Beyond 105 nautical miles from the coast, flow directions reversed, that is, flow was northward in summer and southward in winter.

Geopotential Anomaly and Geostrophic
Flow Off Newport, Oregon

by

Kuo-heng Lee

A THESIS

submitted to

Oregon State University

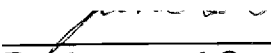
in partial fulfillment of
the requirements for the
degree of

Master of Science

June 1967

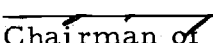
APPROVED:

Redacted for Privacy




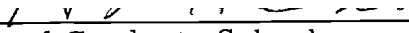
Professor of Oceanography
in charge of major

Redacted for Privacy



Chairman of Department of Oceanography

Redacted for Privacy

Dean of Graduate School

Date thesis is presented April 25, 1967

Typed by Donna Olson for Kuo-heng Lee

ACKNOWLEDGEMENT

I wish to extend my sincere thanks to Dr. June G. Pattullo, my advisor, for her invaluable help and guidance throughout this study.

I am indebted to Dr. Stephen J. Neshyba for his guidance and lectures which provide me a solid background to make this study possible.

My appreciation also goes to Mr. Jackson Blanton for reading and suggestions on the manuscript, and to Mr. William Gilbert for help in preparing the appendix.

Special thanks goes to my wife, Pao Hwa, for her assistance in data processing, typing the original manuscript, and drawing the figures, particularly for her encouragement and unfailing help throughout the entire course of study.

TABLE OF CONTENTS

<u>Chapter</u>	<u>Page</u>
I. INTRODUCTION	1
Scope of Study	1
Previous Studies on the Currents off the Oregon Coast	2
II. HYDROGRAPHIC DATA	5
III. GEOPOTENTIAL ANOMALY	8
Definition	8
Computational Results	9
Thermohaline Effects on Geopotential Anomaly	12
Comparison of Geopotential Anomaly with Oceanic Heat Content	13
IV. GEOSTROPHIC FLOW	17
Method for Computing Geostrophic Flow	17
Reference Level	18
Computational Results	20
Comparison of Geostrophic Computation with Drogue Measurements	29
V. DISCUSSION	32
Reliability of Geostrophic Currents	32
Possible Factors and Errors Affecting the Geostrophic Computation	32
VI. SUMMARY AND CONCLUSIONS	37
BIBLIOGRAPHY	38
APPENDIX	40

LIST OF FIGURES

<u>Figure</u>	<u>Page</u>
1. Annual and seasonal average of geopotential anomaly (surface over 1,000 decibars).	10
2. Seasonal variation of geopotential anomaly for each station (surface over 1,000-dbs).	11
3. Geopotential anomaly (surface over 1,000-dbs) and heat content (offshore average).	15
4. Relationship between geopotential anomaly and heat content.	16
5. Meridional geostrophic currents relative to 1,000 decibars in cm/sec.	25
6. Correlation between geostrophic computation and drogue measurements.	31

LIST OF TABLES

<u>Table</u>	<u>Page</u>
I. Hydrographic cruises used for geostrophic computations off Newport, Oregon.	6
II. Meridional geostrophic current relative to 1,000 decibars in cm/sec.	22
III. Comparison of geostrophic currents with currents measured by drogues.	30

GEOPOTENTIAL ANOMALY AND GEOSTROPHIC FLOW OFF NEWPORT, OREGON

I. INTRODUCTION

Scope of Study

This paper is primarily a study of the geopotential anomaly and geostrophic flow off the Oregon Coast, covering the area from 65 to 165 nautical miles from Newport, Oregon ($44^{\circ}39'$ N latitude, $125^{\circ}35'$ to $128^{\circ}55'$ W longitude). For the sake of simplicity, the Newport Hydrographic Coordinates will be used in this paper to indicate the location of study. For example, stations 65 and 85 nautical miles off Newport are referred to as NH 65 and NH 85 respectively.

The average geopotential anomaly relative to 1,000 decibars and its seasonal and spatial variations are plotted and discussed. The relationship between geopotential anomaly and oceanic heat content is examined.

The monthly average meridional component of the geostrophic flow and its seasonal variation at the depths of 0, 100, 200, 500, 800 meters are computed. In order to verify the dynamic computation, a comparison with the results obtained by direct drogue measurement is made. The reliability of geostrophic computation and the factors which affect this computation are intensively discussed. The errors involved in computing the geostrophic flow in this paper are also estimated.

Previous Studies of the Currents Off the Oregon Coast

According to Sverdrup, Johnson and Fleming (1942), the major current that effects the Oregon Coast is the California current which is a portion of the eastern boundary current system in the North Pacific Ocean.

Wooster and Reid (1960) have studied eastern boundary currents and have concluded that these currents are characterized as slow, broad, and shallow, with relatively small transport. One of the striking features off the Oregon Coast is the upwelling phenomenon. During the spring and early summer months, wind from the north to north-west prevails along the coast of Oregon. These winds give rise to coastal upwelling that begins in May or June and continues until early fall. Sverdrup et al. (1942) stated:

During the entire season of upwelling, a counter-current that contains considerable quantities of equatorial water flows close to the coast at depths below 200 meters. In the fall the upwelling ceases and in the surface layers a current opposite to the direction of the California current develops, the Davidson Current which in December and January runs north along the coast to at least latitude 48° North.

These statements pertain specifically to the California Coast, and to average or prevailing conditions. Details of the circulation off Oregon, and the variability from year to year, or even month to month still need study.

Pattullo and Stevenson (1966) have intensively studied the currents off the Oregon Coast by direct measurement with drogues, and they concluded that subsurface water off the Oregon Coast is influenced by the California Current. The mean flow of surface and subsurface water is southward through the year. The pycnocline, present at 100-200 m, has no apparent effect on north-south flow. Above the pycnocline, the transport is eastward. East-west flow is evidently linked to the density structure. A northward water flow of surface water was noted from several measurements. This flow is probably associated with the Davidson Current.

Burt and Wyatt (1964) studied the surface current by drift bottles and concluded that the northward flowing Davidson Current was observed from October through March. Varying surface currents from both north and south were present during the spring (April and May) and fall (September) transition periods. During the summer (June, July and August), the surface current was toward the south. The Davidson Current varied in width to over 165 miles and was observed to flow as far north as 50° North latitude. The Davidson Current off Oregon appeared to be the direct result of local wind stress.

The upwelling along the Oregon Coast was studied by Smith, Pattullo and Lane (1966). The offshore transport during an early stage of coastal upwelling off the southern coast of Oregon was

computed to be 4.4×10^9 g/cm for the 76-hour period. The vertical velocities computed from the change in depth of the $25.5 \sigma_t$ surface, which is representative of the upper part of the pycnocline off Oregon, decrease linearly from 7.0×10^{-3} cm/sec at the inner station to 0.2×10^{-3} cm/sec at the outer station.

Maughan (1963) studied currents off the Oregon Coast at $44^{\circ}39'N$, $125^{\circ}20'W$. He made comparisons of the data obtained by drogue measurement and by drift bottles. In his discussion, he said:

A great variability appears in the speed of the average surface currents for any given month. For example, from observations of ship-drift during May, the average speed of the surface currents is shown to be about 19 cm/sec, whereas, from direct measurements with drogues, the average current was about 2 cm/sec. Thus, the absolute speed of any given surface current measurement depends not only on the month of observation, but also is highly dependent on other factors, probably the particular weather system that is present during the period of observation.

In this paper the author has computed the average monthly current speed from four years of hydrographic data in order to give some general idea of the mean currents off the Oregon Coast.

II. HYDROGRAPHIC DATA

The hydrographic data used in this paper are listed in Table 1. These data were taken from February, 1962 to December, 1965. There were a total of twenty-one hydrographic cruises which included four cruises each in February and July; three cruises in December; and two cruises each in April, May, June, September and November. In January, March, August and October no Oregon State University data were deep enough for computation relative to the selected reference level which is 1,000 meters. The hydrographic data used were taken from NH 65 to NH 165 with a spacing interval of twenty nautical miles, namely, NH 65, NH 85, NH 105, NH 125, NH 145 and NH 165. From the temperature and salinity observations, the dynamic heights were computed; in turn the geopotential anomaly, and geostrophic flow, were computed. The monthly average of dynamic height is the arithmetic mean value for the same month of different years.

The temperature and salinity distributions are illustrated in the appendix. Pattullo and Denner (1965) have studied the temperature and salinity distribution off the Oregon Coast. Using the data from 1961 to 1962, at stations between 5 and 25 nautical miles offshore, they found that the temperature ranged from 6 to 17°C with a mode between 10 and 11°C. Salinity varied from 18.0 to 33.5‰ with

Table I. Hydrographic cruises used for geostrophic computations off Newport, Oregon.

Month	Year				Monthly Total
	1962	1963	1964	1965	
January					
February	X	X	X	X	4
March					
April	X		X		2
May	X	X			2
June	X			X	2
July	X	X	X	X	4
August					
September	X	X			2
October					
November		X		X	2
December	X	X		X	3
Total					21

a mode between 32.5 and 33.0‰.

During 1963 to 1965, between the coast and 165 nautical miles offshore, temperatures ranged from 18.5 to 3.4°C. Salinities varied from 33.60 to 28.50‰. The modes of temperature and salinity in the upper 200 m were very close to the values calculated by Pattullo and Denner.

Temperature decreases and salinity increases rapidly in the upper layer (about upper 200 meters). Below 200 meters all gradients are small. At 500 meters the temperature decreases to 5 to 5.5°C and the salinity increases to 34.1 to 34.2‰. At 1,000 meters, the temperature is about 3.5°C and salinity is about 34.4‰. The variation below 1,000 meters is practically negligible.

The spatial variations of temperature and salinity from 5 to 165 nautical miles offshore are primarily due to local processes--upwelling, rainfall, and river run-off. From May to September water upwells from a depth of about 200 meters which makes shelf water cold and more saline near the coast. During February and March the river run-off reduces salinity near the coast.

III. GEOPOTENTIAL ANOMALY

Definition

In oceanography, a surface which is at right angle to the direction of gravity is called a level surface. This surface is also called a geopotential surface or gravitational equipotential surface.

The anomaly of the geopotential distance between two isobaric surfaces p_1 and p_2 , or abbreviated as geopotential anomaly, is computed by the following equation (Sverdrup et al., 1942, p. 409)

$$\Delta D = \int_{p_1}^{p_2} \delta \, dp$$

Where:

ΔD = Geopotential anomaly in dyn meters between two isobaric surfaces p_1 and p_2 expressed in decibars

δ = Specific volume anomaly in m^3/kg

$$= \alpha_{S, T, P} - \alpha_{35, O, P}$$

$\alpha_{S, T, P}$ = Specific volume at given salinity, temperature, and pressure

$\alpha_{35, O, P}$ = Specific volume at 35 parts per mille salinity, 0°C temperature, and pressure P

Computational Results

The geopotential anomaly off Newport, Oregon from NH 65 to NH 165 is computed using the 1,000 decibars surface as reference level. The annual, seasonal and monthly average of geopotential anomaly as shown in Figure 1 and Figure 2.

The annual average geopotential anomaly was 1.31 dyn meters, for the entire section, the spatial variation was less than 1 dyn cm.

In summer, which was selected to include data during June, July and September, the geopotential anomaly ranged from 1.37 to 1.32 dyn meters. The maximum value was at NH 105 and the minimum at NH 65.

In winter, which includes data during December and February, the geopotential anomaly was almost uniform at 1.30 except at NH 65 where a maximum value of 1.32 dyn meters occurred.

In spring, including data during April and May, the geopotential anomaly varied from 1.29 to 1.26 dyn meters. Maximum values occurred at NH 65 and NH 165, minimum values at NH 105.

The seasonal variation varied from 1.39 to 1.25 dyn meters. As a whole, the highest geopotential anomaly occurred in summer, especially September, and the lowest anomaly in spring, usually April. In general, the summer anomaly is three dyn cm higher than the annual average, and eight dyn cm higher than the spring average.

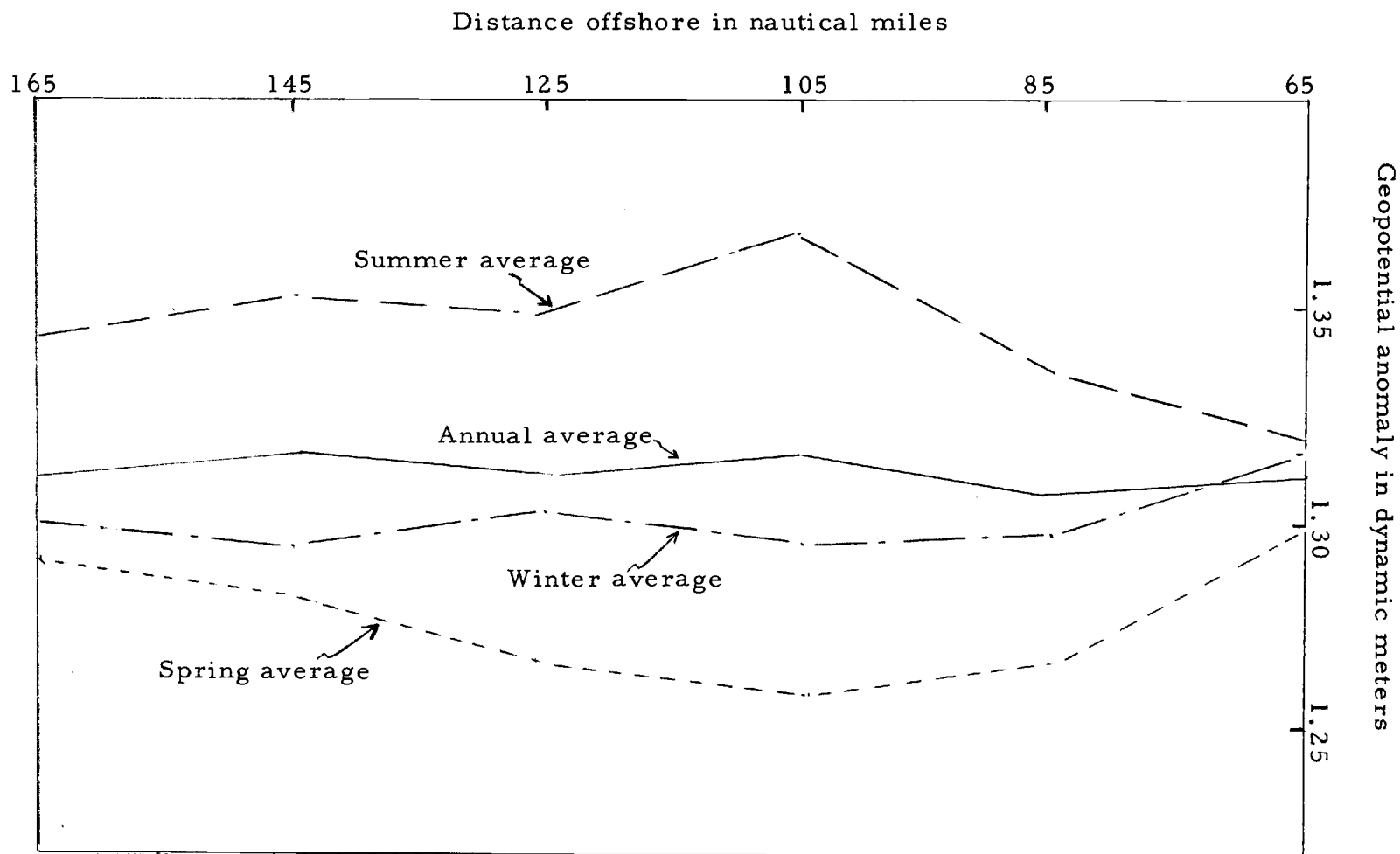


Figure 1. Annual and seasonal average of geopotential anomaly (surface over 1,000 decibars).

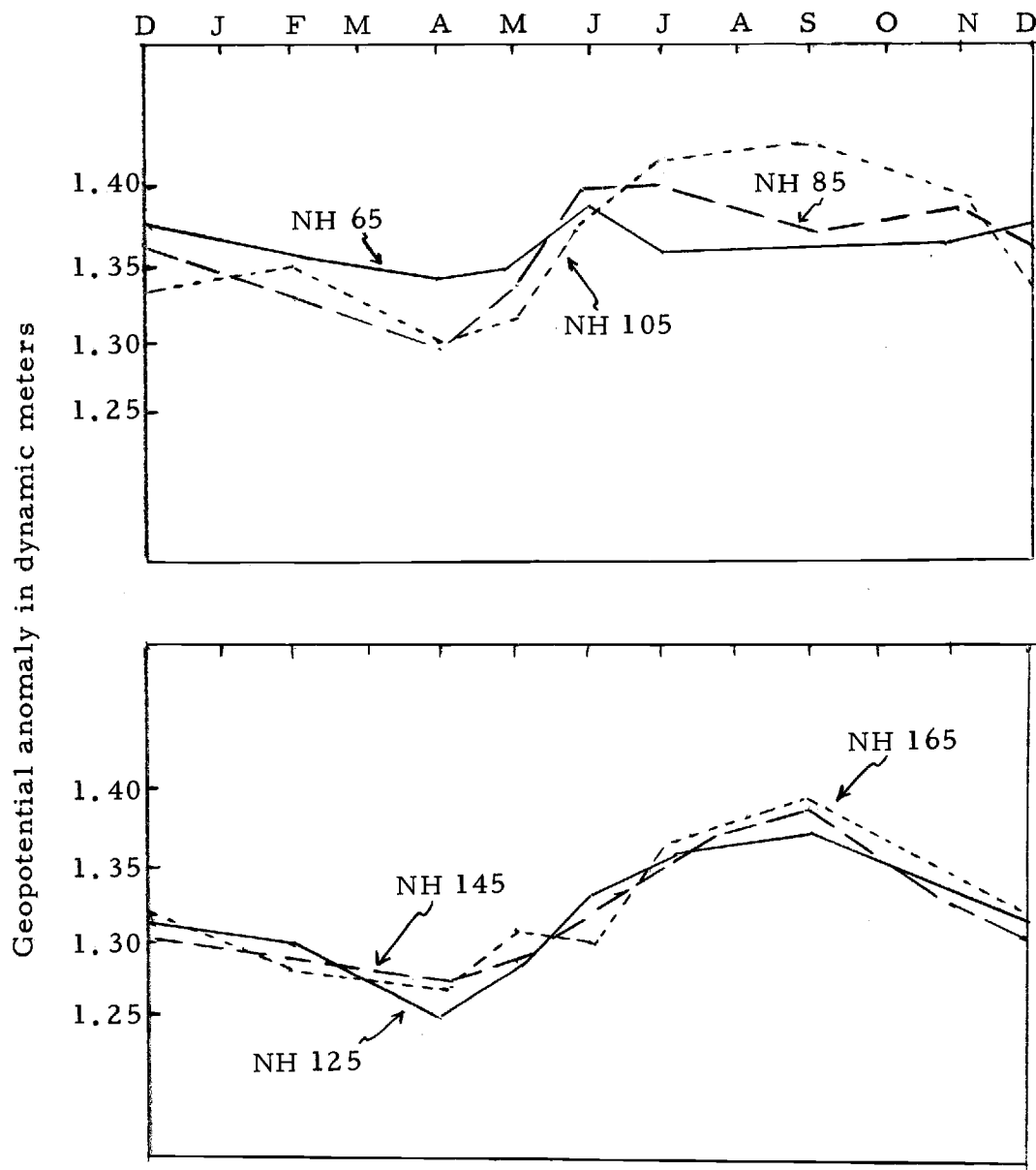


Figure 2. Seasonal variation of geopotential anomaly for each station (surface over 1,000-dbs).

The seasonal variation was a maximum at NH 105 with a magnitude in the order of 14 dyn cm.

The most striking feature discovered from the computations was that the lowest surface geopotential anomaly occurred in spring rather than in the winter. This is primarily related to the oceanic heat content. It seems that the upwelling occurring in late spring plays an important role in affecting the geopotential anomaly.

The geopotential anomaly with minimum values in April, increased as time went on, and reached its peak value in September, then decreased again until April. This annual oscillation appeared to be related to, as aforementioned, heat content and thermosteric effects which will be discussed in detail in a later section.

Thermohaline Effects on the Geopotential Anomaly

The thermohaline effects have been studied by Pattullo et al. (1955). The relationship they found between geopotential anomaly and thermohaline effects is expressed approximately by the formulas:

$$Z_T = g^{-1} \int_{p_a}^{p_o} (\partial \alpha / \partial T) \Delta T \, dp \quad \text{and}$$

$$Z_S = g^{-1} \int_{p_a}^{p_o} (\partial \alpha / \partial S) \Delta S \, dp$$

where

Z_T = thermal departure from annual mean geopotential
anomaly

Z_S = haline departure from annual mean geopotential anomaly

p_a = atmospheric pressure

p_o = the pressure to which the integration carried

For any depth let $\Delta T = T - \bar{T}$, and $\Delta S = S - \bar{S}$ designate the monthly departures in temperature and salinity from their annual means, \bar{T} , \bar{S} . For small values of ΔT and ΔS the corresponding departure in specific volume is given by

$$\Delta \alpha = \alpha(T, S, P) - \alpha(\bar{T}, \bar{S}, P).$$

$$= (\partial \alpha / \partial T) \Delta T + (\partial \alpha / \partial S) \Delta S + \dots$$

Where $\partial \alpha / \partial T$ and $\partial \alpha / \partial S$ are to be evaluated at T , S , P .

But the explicit dependence of $\partial \alpha / \partial T$, $\partial \alpha / \partial S$ on pressure can be neglected, and accordingly in all numerical work $\partial \alpha / \partial T$ and $\partial \alpha / \partial S$ may be read as functions of $\bar{T}(p)$, $\bar{S}(p)$, O .

Comparison of Geopotential Anomaly with Oceanic Heat Content

A comparison of geopotential anomaly and heat content has been made and shown in Figure 3 and Figure 4.

The oceanic heat content in the upper 100 m off Newport, Oregon has been studied by Burt, Pattullo and Kulm (in preparation) with the hydrographic data from 1962 to 1965 (the same data used

in this paper for computing the geopotential anomaly).

Figure 3 shows that the two results are very closely correlated. The seasonal variation of upper layer heat content and geopotential anomaly followed the same trend, and in both cases, the lowest values occurred in April and the highest values in September.

Geopotential anomaly versus surface heat content (NH 105 - 165) is shown in Figure 4. The straight line is obtained by regression analysis. The simple positive correlation between heat content and geopotential anomaly has been calculated as 3.1×10^{-1} dyn cm/kg cal/cm². The result showed that the relationship between geopotential anomaly and surface heat content is indeed linear. It also suggests that the specific volume anomaly off the Oregon Coast is primarily influenced by the heat content of the upper layer.

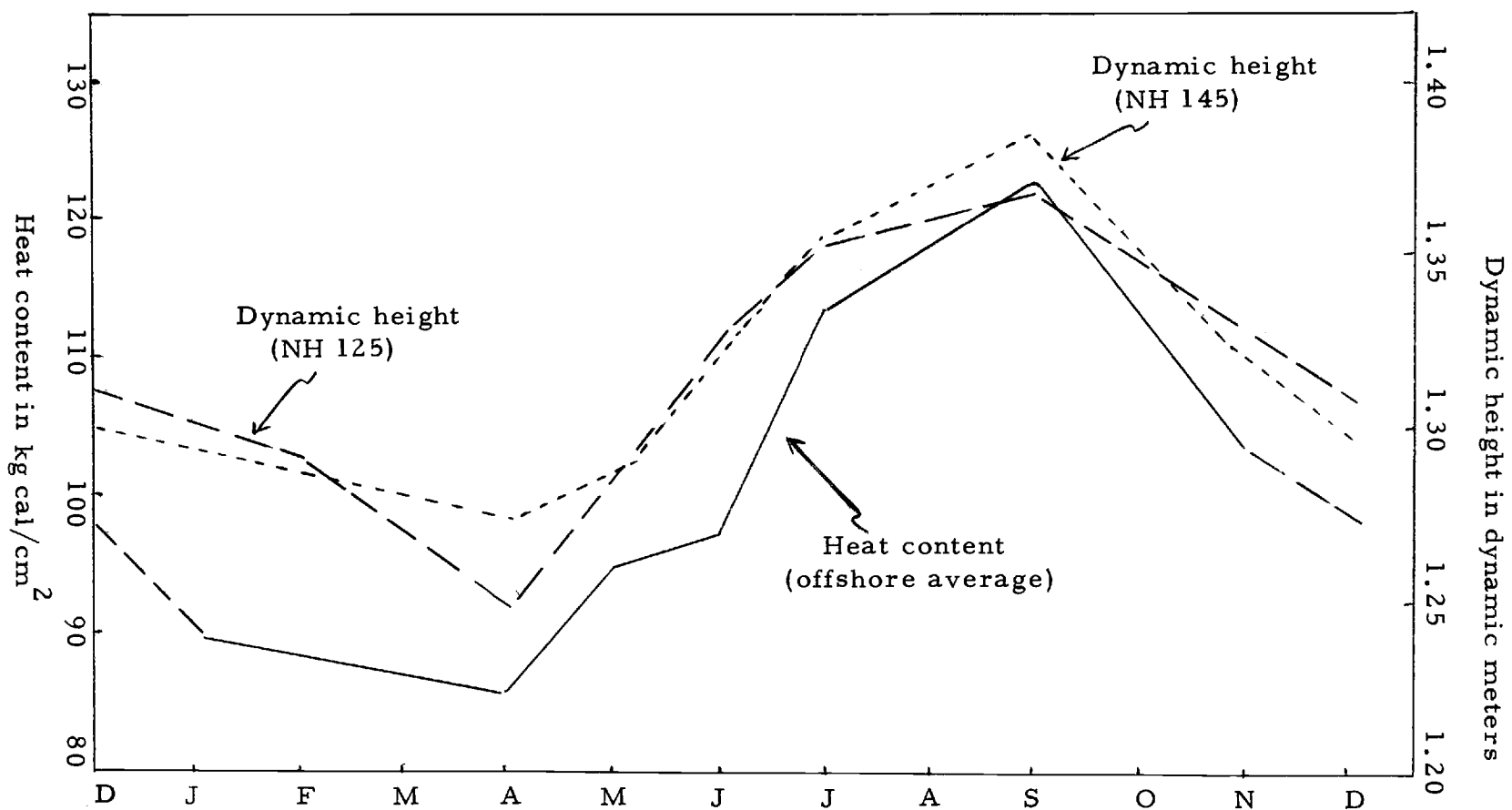


Figure 3. Geopotential anomaly (surface over 1,000-dbs) and heat content (offshore average).

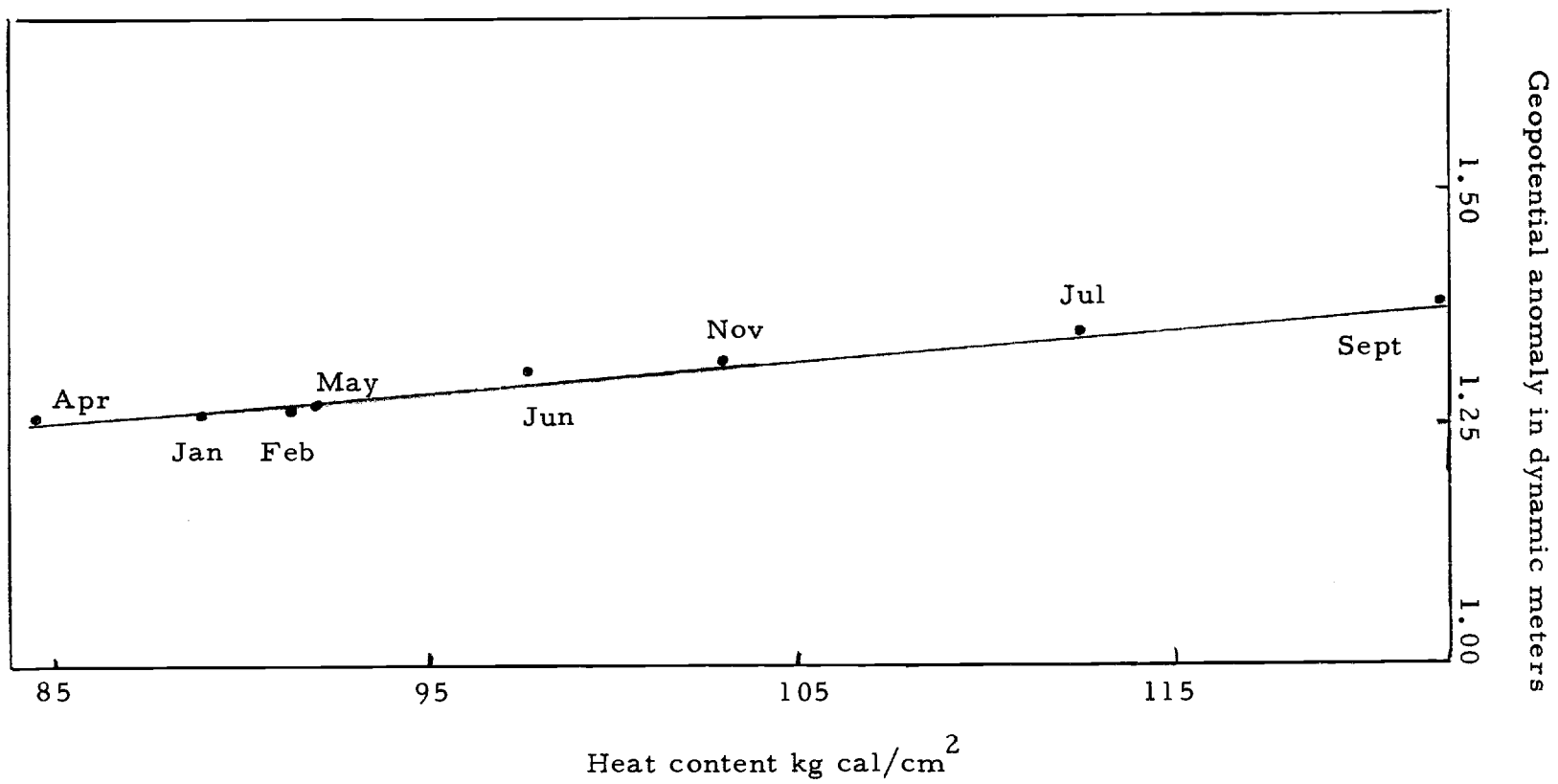


Figure 4. Relationship between geopotential anomaly and heat content (see Figure 3).

IV. GEOSTROPHIC FLOW

Method for Computing Geostrophic Flow

Permanent ocean currents can be computed from the observed distribution of density on the assumptions that: (1) the horizontal pressure gradient is balanced by the coriolis force (2) the horizontal velocity and the horizontal gradient vanish at a moderate depth below sea surface (3) the acceleration and frictional force are neglected. Those assumptions simplify the equation of motion into the so called geostrophic equation (Sverdrup, 1947)

$$\frac{1}{\rho} \frac{\partial p}{\partial x} = fu \quad (1)$$

$$\frac{1}{\rho} \frac{\partial p}{\partial y} = -fv \quad (2)$$

The relative current between two isobaric surfaces is given by the equation

$$V_1 - V_o = \frac{10 (\Delta D_A - \Delta D_B)}{f \cdot L} \quad (3)$$

Where

V_o = Current velocity at the reference level

V_1 = Current velocity at a given level

ΔD_A = Geopotential anomaly at hydro-station A

ΔD_B = Geopotential anomaly at hydro-station B

f = Coriolis parameter

L = Distance between the two hydrographic stations

The monthly average value of current speed is obtained by using the monthly average of ΔD , substituted into equation (3).

Reference Level

The 1,000 decibar surface was chosen as the reference level for the computations in this paper. This is partly due to the availability of hydrographic data, which were mostly taken down to 1,000 meters. However, using Defant's method, the 1,000 decibar surface seems close to the depth of no motion off the Oregon Coast.

Fomin (1964) studied various methods in determining the depth of no motion and concluded that of the existing methods for determining the depth of no motion, the best are that of A. Defant and H. Sverdrup's method. The Defant's method was summarized by Fomin as follows:

From analysis of the differences in the dynamic heights of isobaric surfaces at a great number of pairs of neighboring stations, A. Defant (1941) discovered a layer of relatively great thickness in which these differences vary considerably along the vertical. The thickness of this layer in the Atlantic Ocean ranges from 300 to 800 meters and its depth varies rather uniformly in the horizontal direction, while the change in differences in the dynamic heights of isobaric

surfaces only amounts to several dynamic millimeters. The constancy of differences in dynamic heights indicates that the gradient component of current velocity is constant along the vertical in this layer. Defant assumes that this water layer is almost motionless and considers it to be the layer directly adjoining the 'zero surface'.

Using Defant's method, the depth of no motion off Newport, Oregon was found to be at 600 to 800 meters depth approximately. Since the hydrographic data used to compute the depth of no motion were mostly taken down only to 1,000 meters, there is no way to detect the depth of no motion below 1,000 meters.

According to Wooster and Reid (1960) the principal equatorward flow of the Pacific eastern boundary currents is above 1,000 meters and in most places is above 500 meters. Furthermore, their transport calculations relative to the 1,000-db or 2,000-db surfaces show little difference. Wooster and Reid also computed the transport of various Pacific eastern boundary currents. The results show that the choice of reference level below 1,000-db seems to make little difference to the computed values with respect to 1,000-dbs.

McAlister (1962) has examined the depth of no motion in the North Pacific with the data down to 5,000 meters. The depth of no meridional motion that McAlister computed was at about 1,000 meters in the area along 48°N . and between 130°W . to 150°W . That is close to the area studied in this paper.

Therefore, it seems reasonable to believe that the depth of no

motion off Newport, Oregon is at some depth around 1,000 meters. In other words, the depth of 1,000-dbs chosen for the dynamic computations in this paper seems to be an adequate approximation.

Computational Results

The results of the meridional geostrophic currents relative to 1,000 decibars off Newport, Oregon are shown in Table 2 and illustrated in Figure 5. The computed geostrophic currents generally were weak and irregular.

The surface currents mostly ranged from 2 to 6 cm/sec. The maximum speed computed was 21 cm/sec between stations NH 85 and NH 105 in September. Several times speeds over 10 cm/sec appeared in April and July.

For sake of convenience in generalizing the currents in the whole area, stations NH 65 - NH 105 ($125^{\circ}35'$ to $126^{\circ}31'$ W. longitude) are classified as the inshore area, and NH 105 - NH 165 ($126^{\circ}31'$ to $128^{\circ}55'$ W. longitude) as the offshore area.

Through the year, inshore average currents were stronger than those offshore. Inshore current speeds ranged from 3 to 12 cm/sec except for a couple of very weak currents in April and May. Offshore current speeds ranged from 1 to 5 cm/sec. Generally, the current speed tended to decrease with depth.

The current direction was irregular. Sometimes the flow

reversed direction at every station. This result is primarily due to the fact that the difference of geopotential anomaly between two adjacent hydrographic stations was so small that the differences are uncertain, since the geopotential anomaly difference, from which the geostrophic currents are computed, are uncertain to 0.01 dyn meters (Smith, 1964). The geostrophic current will be uncertain, if the magnitude of currents are less than the order of 2.6 cm/sec. (Note: In the latitude $44^{\circ}39'$ N. with station spacing of 20 nautical mile, the geostrophic current is in the order 2.6 cm/sec when $\Delta D_A - \Delta D_B = 1$ dyn cm.)

More than 50% of the geostrophic currents were less than 2.6 cm/sec. Therefore, it is very difficult to draw any generalizations about the current system in this area.

However, if we ignore currents of small magnitude (less than 2.6 cm/sec), the data show some characteristics in common.

The meridional flow of geostrophic current through the Newport hydrographic section may be summarized as follows:

From June through November inshore average flows were predominantly southward, while offshore average flows were northward.

From December through May, inshore average flows were predominantly northward while offshore flows were southward.

Table II. Meridional geostrophic current relative to 1,000 decibars
in cm/sec. (positive values indicate northward flow)

February

Depth (meters)	NH 65-85	NH 85-105	NH 105-125	NH 125-145	NH 145-165
0	6	-4	1	2	1
100	6	-3	1	3	0
200	5	-3	1	4	2
500	6	-5	1	4	2
800	1	-1	1	1	1

April

0	14	-1	0	-5	-4
100	18	-1	1	-2	-3
200	14	-1	2	-4	-2
500	5	0	2	-2	-2
800	2	0	1	-1	-1

May

0	1	4	-3	-1	-5
100	1	3	0	-2	-4
200	0	1	2	-1	-3
500	1	0	3	-2	-1
800	1	-1	2	-1	-1

Table II. cont.

June

Depth (meters)	NH 65-85	NH 85-105	NH 105-125	NH 125-145	NH 145-165
0	-5	7	2	2	5
100	-3	5	5	-1	2
200	-5	8	5	-2	1
500	0	2	3	-1	1
800	0	3	1	0	0

July

0	-12	-4	5	-1	-2
100	-4	-3	4	-2	0
200	0	-3	2	-1	0
500	0	-2	0	2	-1
800	0	0	1	1	0

September

0	4	-21	3	-5	4
100	6	-7	7	-4	-2
200	5	2	7	-4	-1
500	6	-1	4	-2	0
800	2	0	1	0	-1

Table II. cont.

November

Depth (meters)	NH 65-85	NH 85-105	NH 105-125	NH 125-145	NH 145-165
0	-6	-3	5	3	-
100	-6	1	4	2	-
200	-4	0	5	2	-
500	-2	1	2	3	-
800	1	1	1	0	-

December

0	4	5	-5	3	-4
100	4	3	-4	2	-2
200	5	1	-4	3	-1
500	2	0	-3	3	1
800	1	0	0	0	1

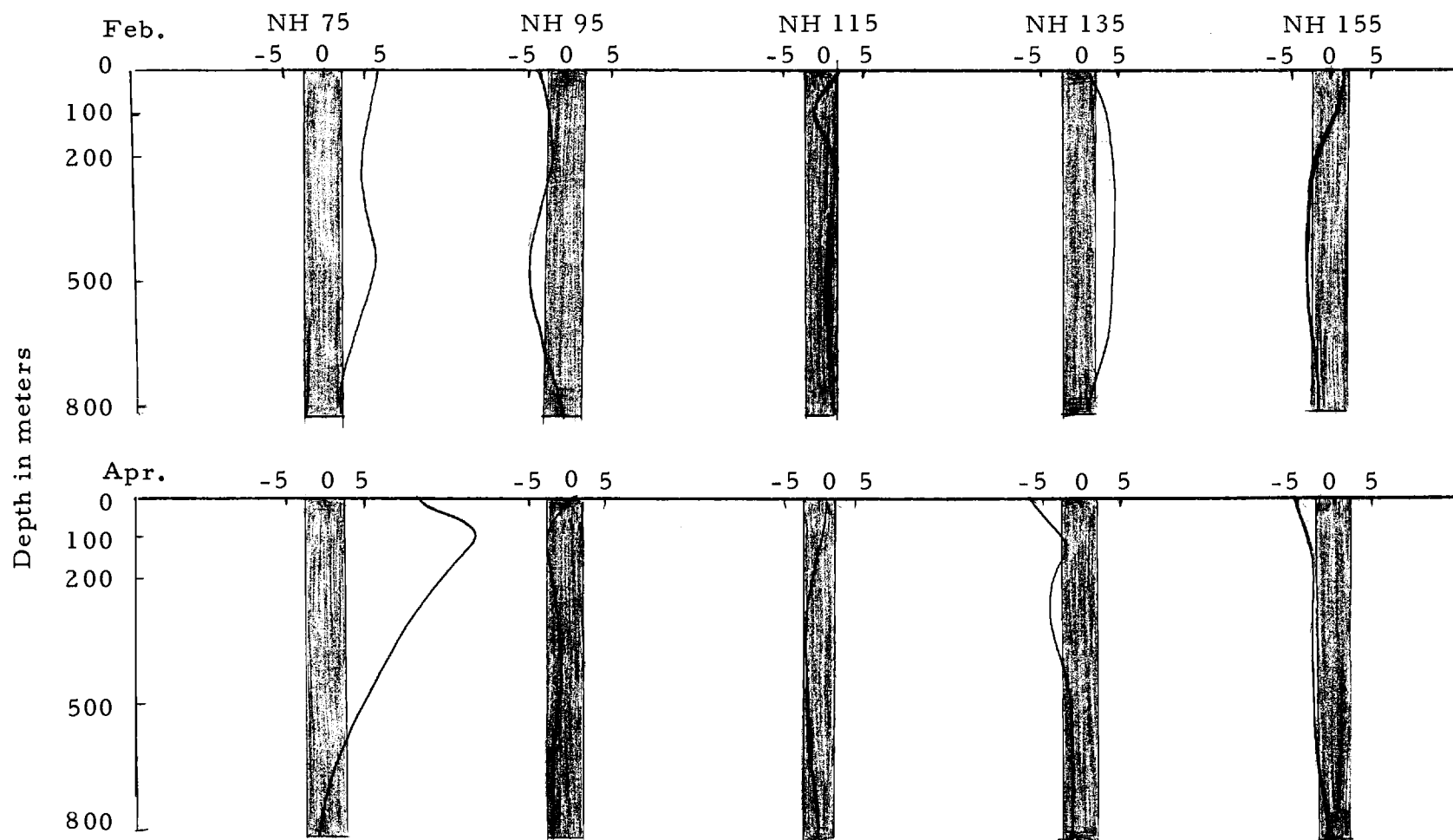


Figure 5. Meridional geostrophic currents relative to 1,000 decibars in cm/sec (positive values indicate northward flow, shading means current of uncertainty).

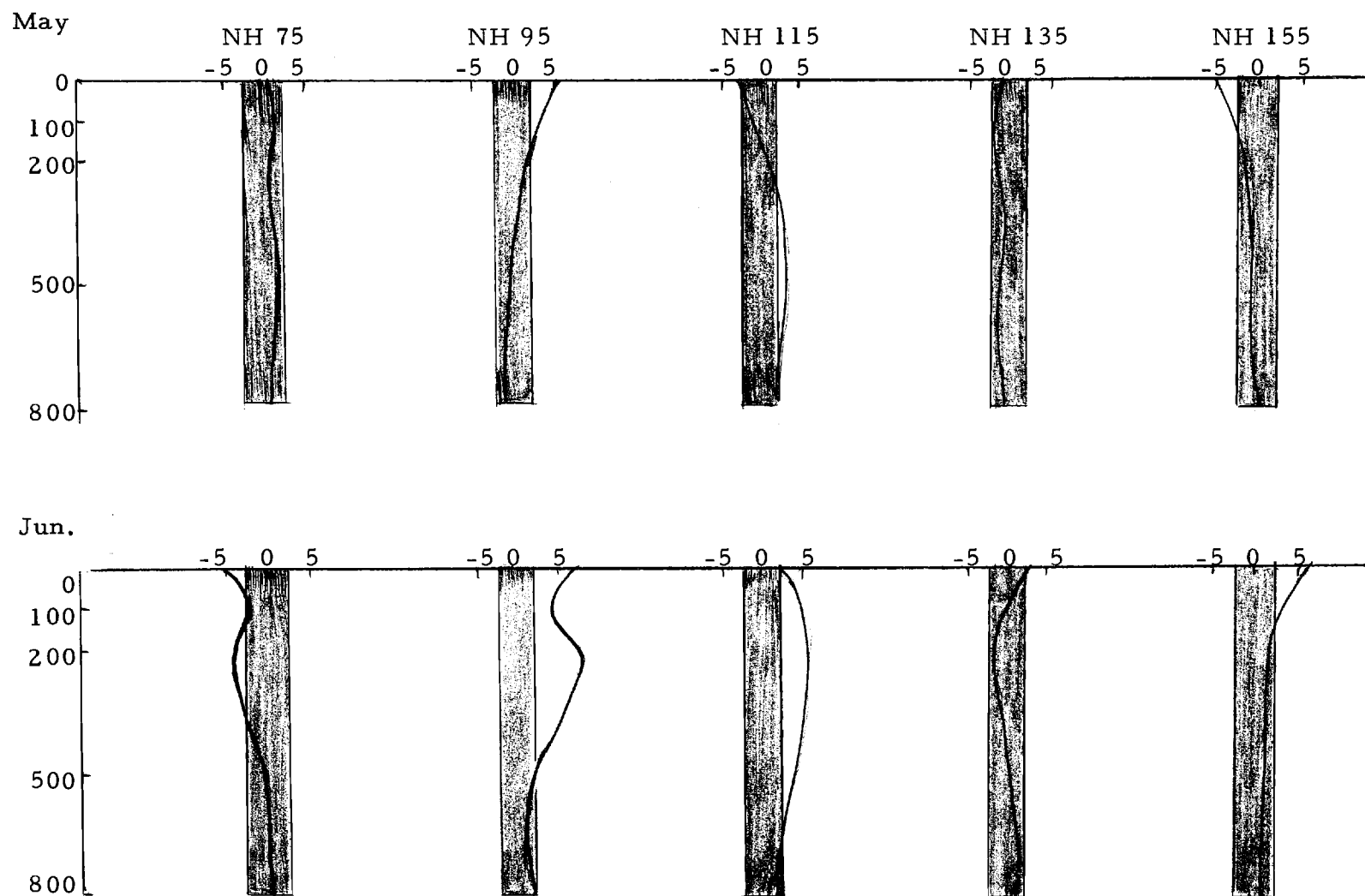


Figure 5. cont.

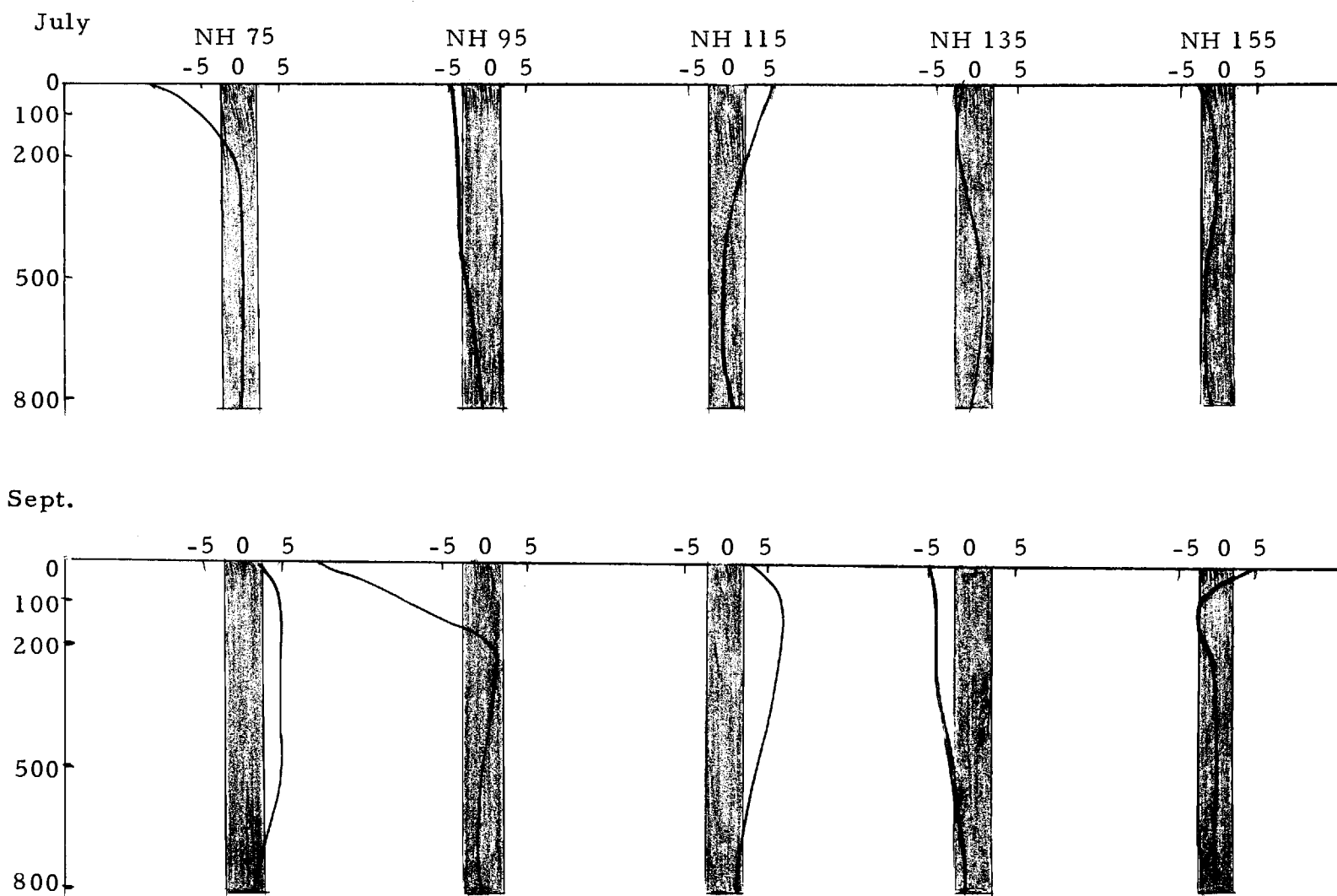
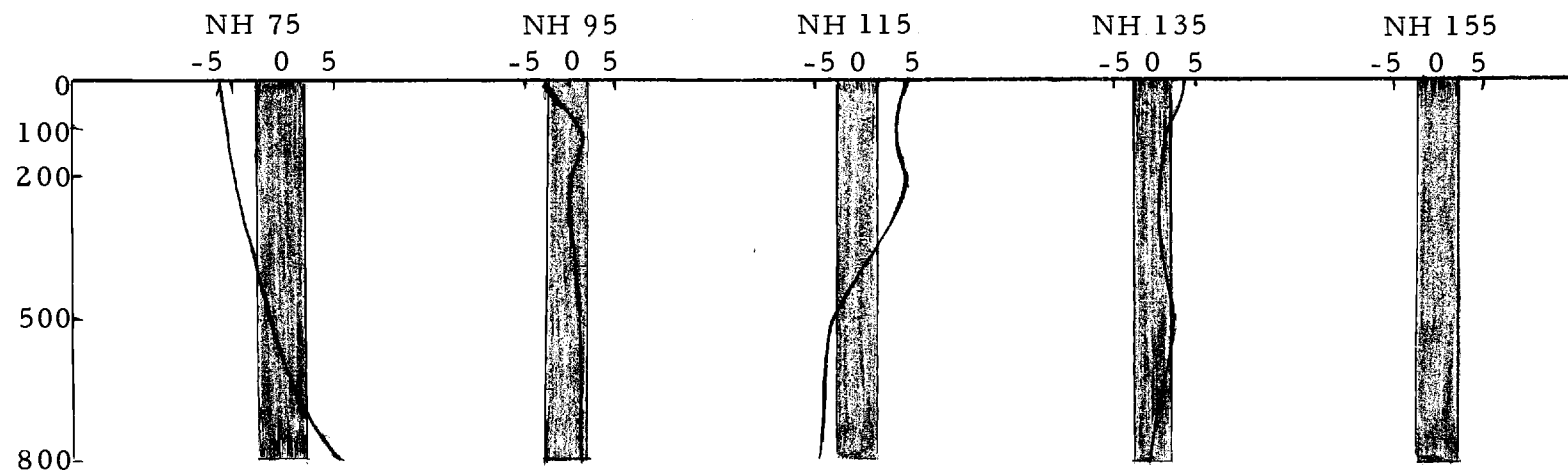


Figure 5. cont.

Nov.



Dec.

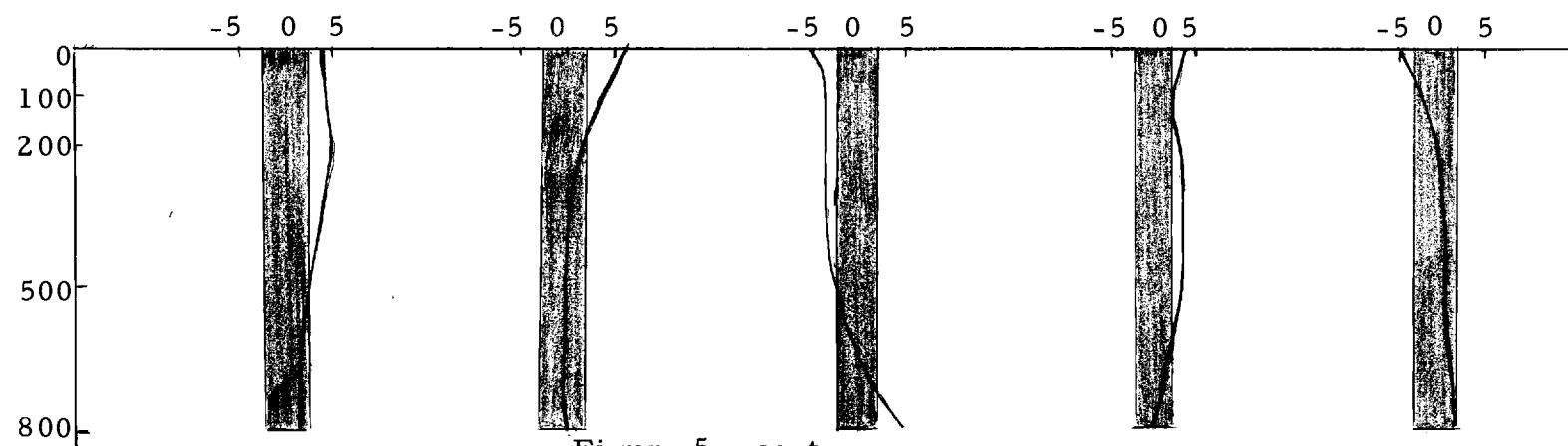


Figure 5. cont.

Comparison of Geostrophic Computation with Drogue Measurements

The currents obtained by geostrophic computation were compared with direct measurements using drogues (Pattullo and Stevenson, in preparation). These are shown in Table 3 and Figure 6.

Table 3 shows that the currents determined by the two methods were generally in agreement with a few exceptions in September and November. However, the great discrepancies occurred during weak currents which are indeterminant by the geostrophic computation. Figure 6 shows the correlation between currents determined by geostrophic computation and by drogue measurements. The correlation coefficient is 0.96. For a one-to-one plot, the slope of correlation line is 43.8° which demonstrates a very good correlation between two methods.

It is noteworthy that the drogue measurements were taken at NH 45, while the hydrocasts, from which the geostrophic currents were computed, were taken between NH 65 and NH 85. The distance between two measurements was twenty or thirty nautical miles. Furthermore, the drogue measurements and hydrocasts were taken in the same month, but the dates were different. This leads to the postulation that in the open ocean (beyond NH 45) the steady currents are somewhat persistent. However, the data are limited, there were only six cruises for which data could be compared.

Table III. Comparison of geostrophic currents with currents measured by drogues.

	Meridional Component of Drogue Measurement (at NH 45)	Computed Meridional Geostrophic Current (At NH 65-NH 85)
	May 31, 1962	May 2, 1962
0 m	-1.39	-0.26
100 m	+0.79	+0.79
200 m	+1.39	+2.37
	July 5, 1962	July 27, 1962
0 m	-13.92	-19.01
100 m	- 6.70	-10.56
200 m	-10.86	- 5.81
	July 11, 1965	July 15, 1965
0 m	-20.2	-18.00
100 m	- 7.6	- 8.70
200 m	- 6.1	- 2.64
500 m	- 3.6	- 1.58
	Sept 24, 1962	Sept 5, 1962
0 m	- 2.04	+ 0.26
100 m	+ 0.60	- 1.05
200 m	+ 3.59	- 0.52
	Nov 17, 1962	Nov, Average
0 m	-13.87	- 5.81
100 m	- 3.28	- 5.54
200 m	- 4.52	- 3.69
	Dec 17, 1964	Dec, Average
0 m	+ 5.80	+ 3.96
100 m	+ 0.30	+ 3.69

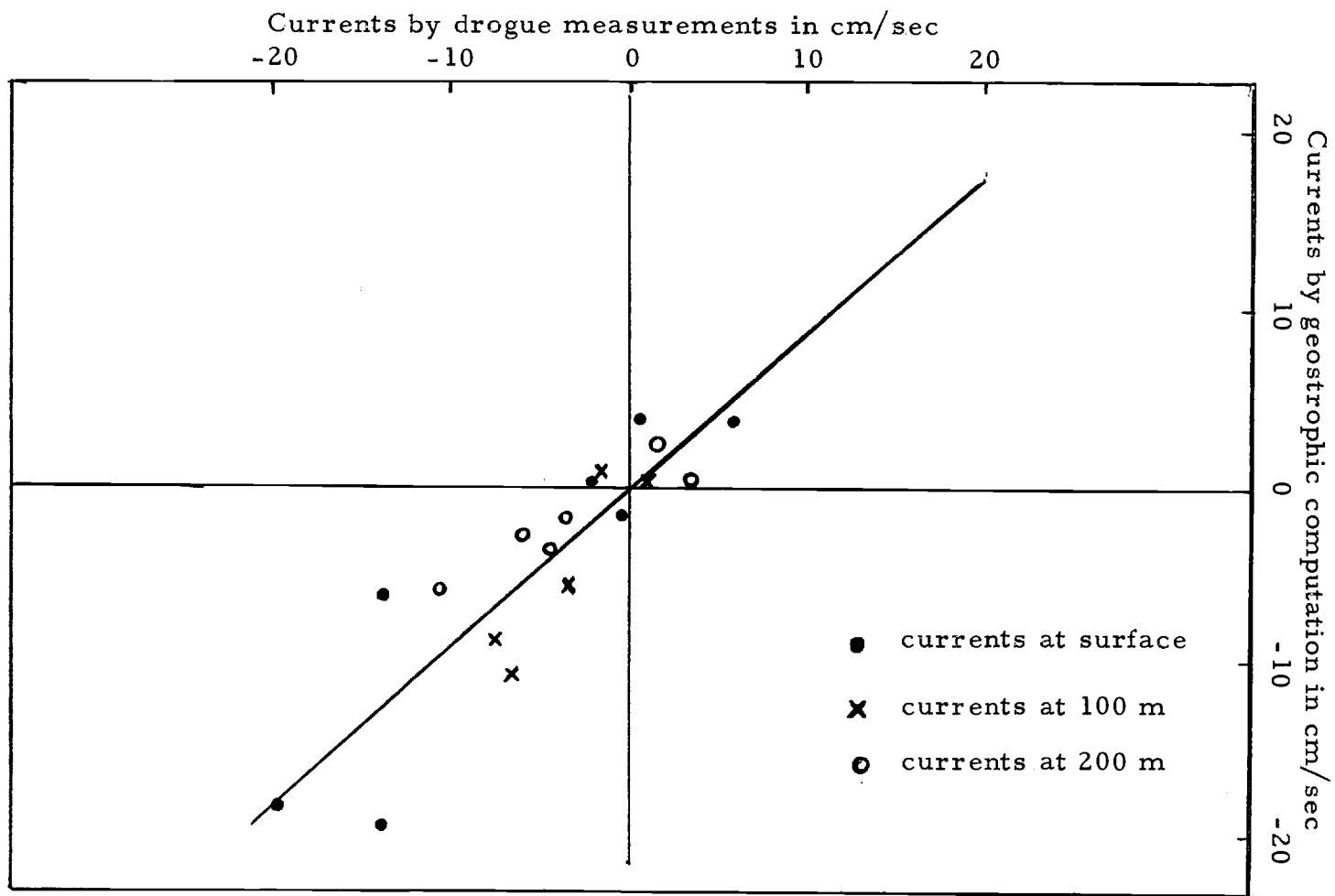


Figure 6. Correlation between geostrophic computation and drogue measurements.

V. DISCUSSION

Reliability of Geostrophic Currents

The reliability of geostrophic computation had been studied by Van Arx (1962) as follows:

Comparison of direct measurements of flow observed by Pillsbury (1890) in the Straits of Florida, with dynamic sections computed by Wüst (1924), for the same area show that the relative field of motion obtained from dynamic sections, using Pillsbury's observed surface of no motion, lead to substantially the same results. Further comparisons of the field of motion inferred from the distribution of density by means of the geostrophic approximation have been made by the International Ice Patrol and by the Meteor expedition. In these cases, it found that the current observed by direct methods may depart from the geostrophic field of motion by amounts which range from 5% to 25%, with the mean departure in the neighborhood of 15%. Studies of the effects of curvature on the transport of the Gulf Stream, using data from the 1950 multiple-ship survey of that current off the coast of New England. These studies show that the difference between the computation based on geostrophic flow and that for meander flow can amount to 15%. However, Parr (1938), in a comparison of isopycnic and geostrophic analysis of the flows of the Labrador Current and the Gulf Stream system south of the Grand Banks of Newfoundland, showed that agreement "would be utterly unobtainable" in some portions of the area. (Von Arx, 1962, p. 254)

Possible Factors and Errors Affecting the Geostrophic Computation

In this paper, the results of dynamic computation showed some

variability in current direction that led to the examination of possible factors which may affect the dynamic computation of geostrophic flow.

Defant (1950) has shown that the errors produced by long-period internal waves are not negligible, and has suggested observational precautions which tend to suppress their influence.

Wooster and Taft (1958) examined the measurement error in the geopotential anomaly of the upper 1,000 m (0/1,000 db) and concluded that the error in anomaly difference between two stations is ± 1.1 dyn cm (two standard deviations). They were aware that the large error due to salinity titration constituted the greater part of the anomaly error. With the modern salinometers, the measurement error still exists ± 0.3 dyn cm as compared to their value of ± 1.1 dyn cm (Reed and Laird, 1966).

Internal waves of near tidal period could produce variations in anomaly greater than those caused by measurement error. Reid (1956) reported 12-hr variations as great as 5 dyn cm at single sites off the California coast but later suggested (1961) that such large fluctuations are rare over most of the Pacific Ocean. According to Reed et al., the measurement error and fluctuations due to waves combine to produce a value very close to the measurement error reported by Wooster and Taft: consequently, ± 1.1 dyn cm will be used as the total error estimate in the anomaly difference

(0/1,000 db) between the two stations.

The Department of Oceanography, Oregon State University, has occupied anchor stations to study the internal wave fluctuation off the Oregon Coast. Data from one such cruise showed that the dynamic height anomaly due to internal wave fluctuation at station NH 65 for a 25-hr period was in the order of ± 1.0 dyn cm (personal communication with Mr. Mooers). If we consider the difference of geopotential anomaly between two stations, we have to take the root mean square value. Then, the anomaly difference between two hydrographic stations will be 1.4 dyn cm (i.e. $\sqrt{2} = 1.4$). That is close to the value 1.1 dyn cm given by Reed (1966) for Pacific area.

Among those factors which affect the geostrophic computation, internal wave effect is the largest. Thus, the geostrophic flow may be completely indeterminate if the difference in geopotential anomaly between two adjacent stations is less than 1.4 dyn cm since this difference $(\Delta D_A - \Delta D_B)$ by which the geostrophic flow is computed, may be outweighed by the internal wave effect. In other words, a geostrophic current less than the magnitude of 3.6 cm/sec will be uncertain. Therefore, the value of 3.6 cm/sec seems to be the critical test value below which the current from geostrophic computation in this paper might be uncertain. However, the dynamic computation in this paper was based on several cruise data. Thus, the internal wave effect should be eliminated to some extent. In

other words, if the computation is based on an average value of N-cruises' data, the critical value should be divided by \sqrt{N} (since standard deviation of the error should be divided by \sqrt{N}).

In this paper, the data used to compute geostrophic flow were varied from four to two cruises (see Table 1), therefore, the critical value should be reduced to 1.8 cm/sec, 2.0 cm/sec, and 2.5 cm/sec respectively. If we round off the decimal point which is insignificant in geostrophic computation, the overall critical testing value becomes 2 cm/sec. Namely, any current computed in this paper less than 2 cm/sec is uncertain.

A second factor affecting the geostrophic computation is the error of positioning induced by the use of Loran. Von Arx (1962) states:

Experience at sea indicates that the standard error in Loran, a fix made in range 300 to 500 miles from transmitters is approximately 0.7 nautical miles.

With the present equipment aboard the R/V Yaquina, and R/V Acona, experience has shown that the average error in positioning with Loran is less than 0.5 nautical mile, which is somewhat better than that stated by Von Arx.

In this paper, the station spacing, L , chosen for geostrophic computation is 20 nautical miles, and the positioning error induced by Loran, dL , is ± 0.5 nautical miles. Then positioning error ϵ_p will be

$$\epsilon_p = \frac{dL}{L} = 0.05 \quad \text{or} \quad 5\%$$

In view of the fact that the geostrophic currents computed in this paper were generally in the order of 5 cm/sec or less, the positioning error induced by Loran can be neglected.

VI. SUMMARY AND CONCLUSIONS

The annual average of geopotential anomaly off Newport, Oregon was 1.31 dynamic meters. The seasonal variation was of the order of 14 dyn cm. The highest value occurred in summer, particularly September, and lowest value occurred in spring, generally April. This feature was primarily related to oceanic heat content in the upper layer. By regression analysis, the geopotential anomaly and oceanic heat content was found to be linear in character, and the correlation computed was 3.1×10^{-1} dyn cm/kg cal/cm².

The currents off the Oregon Coast were weak and irregular. The surface currents mostly ranged 2 to 6 cm/sec with a maximum current speed of 21 cm/sec, and a minimum speed of zero cm/sec. The average magnitude of meridional flow was in the order of 5 cm/sec or less. The direction of meridional geostrophic flow varies with season. From June through November, inshore average flow was southward whereas offshore average flow was northward. From December through May the average inshore flow was northward whereas offshore average flow was southward.

The geostrophic computation was affected by the internal wave fluctuation. A current less than 2 cm/sec was uncertain. The geostrophic computation due to positioning error can be practically neglected. The currents determined by geostrophic computation and drogue measurements were generally in agreement.

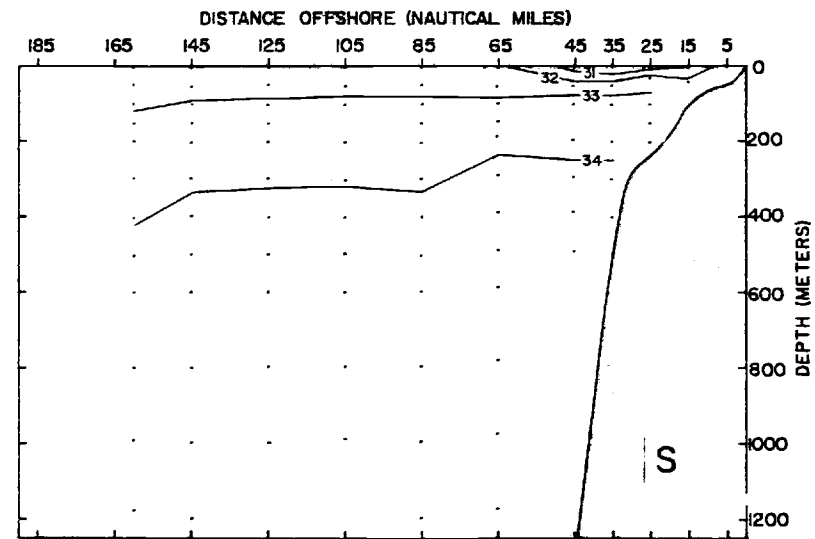
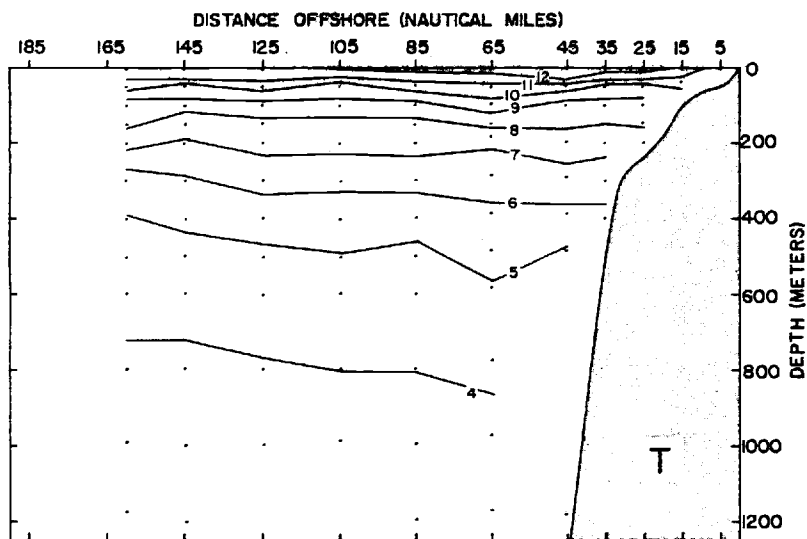
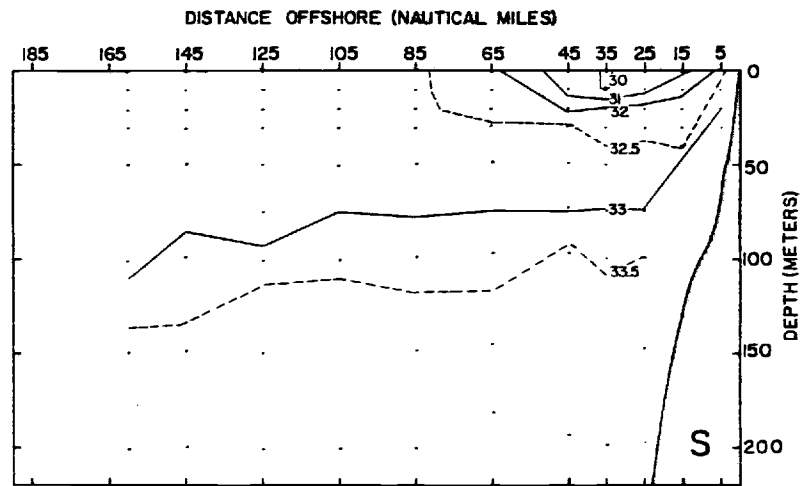
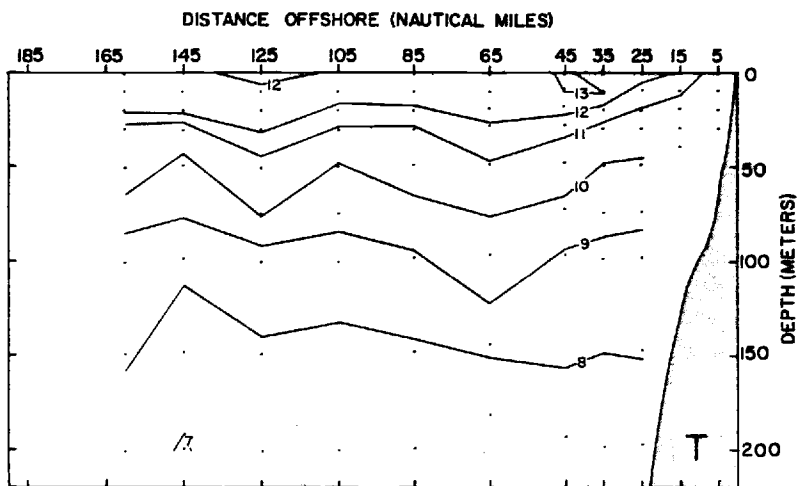
BIBLIOGRAPHY

- Burt, W., J. Pattullo and S. Kulm. 1967. Unpublished research on oceanic heat content off the Oregon Coast. Corvallis, Oregon. Oregon State University, Department of oceanography.
- Burt, W. and B. Wyatt. 1964. Drift bottle observations of the Davidson Current off Oregon. University of Washington, Studies on Oceanography, p. 156-165.
- Defant, Albert. 1961. Physical oceanography. New York, Pergamon. 2 vols.
- Fomin, L. M. 1964. The dynamic method in oceanography. New York, Elsevier. 212p.
- Maughan, Paul M. 1963. Observation and analysis of ocean currents above 250 meters off the Oregon Coast. Master's thesis. Corvallis, Oregon State University. 49 numb. leaves.
- McAlister, William. 1962. The general circulation in the North Pacific Ocean referred to a variable reference surface. Ph.D. thesis. Corvallis, Oregon State University. 69 numb. leaves.
- Pattullo, J. and W. Denner. 1965. Processes affecting seawater characteristics along the Oregon Coast. Journal of Limnology and Oceanography 10 (3):443-450.
- Pattullo, J., M. Munk, R. Revelle and E. Strong. 1955. The seasonal oscillation in sea level. Journal of Marine Research 14 (1):88-121.
- Reed, R. K. and N. R. Laird. 1966. On the reliability of geostrophic flow determinations across a section of the North Pacific Ocean. Paper presented at the Pacific Northwest Regional Meeting of the American Geophysical Union. Corvallis, Oregon.
- Reid, J. L., Jr. 1956. Observation of internal tides in October 1950. Transactions of the American Geophysical Union 37 (3):278-286.

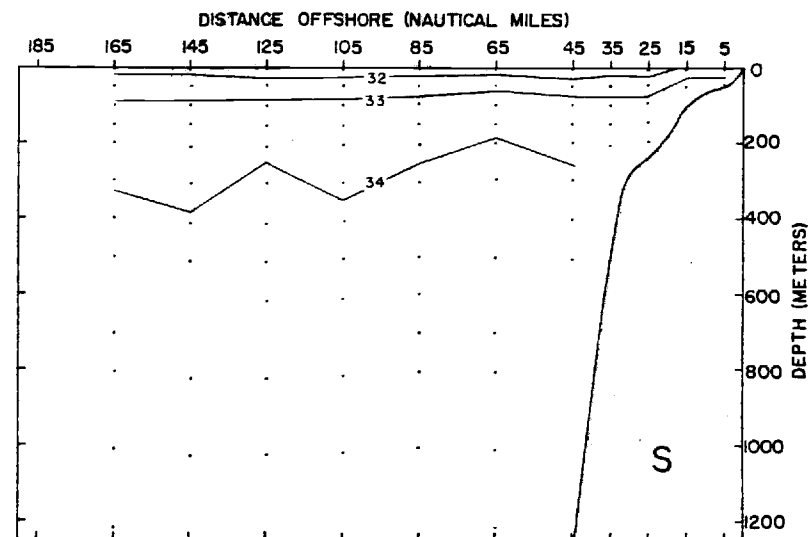
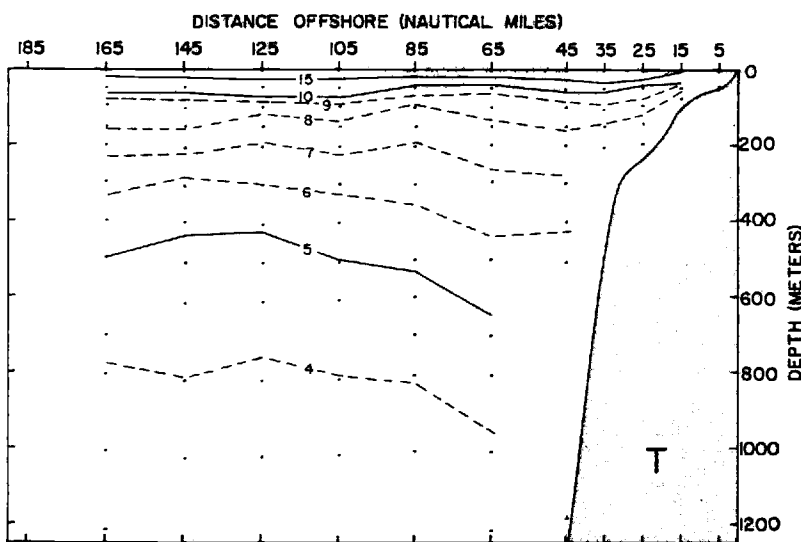
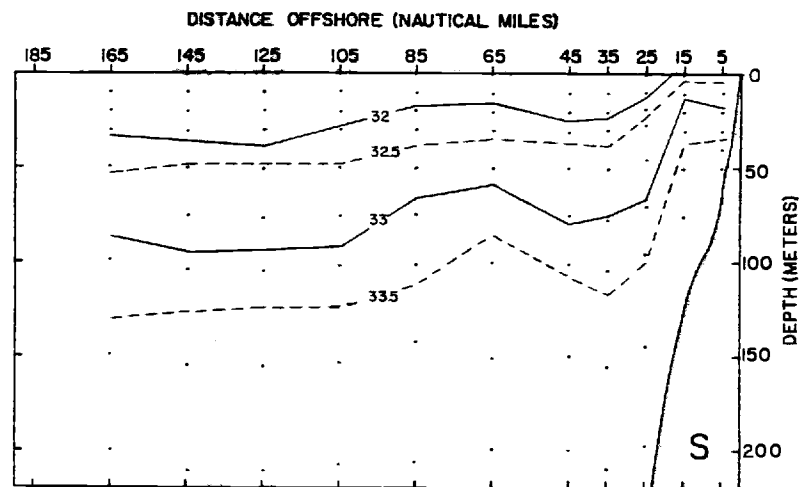
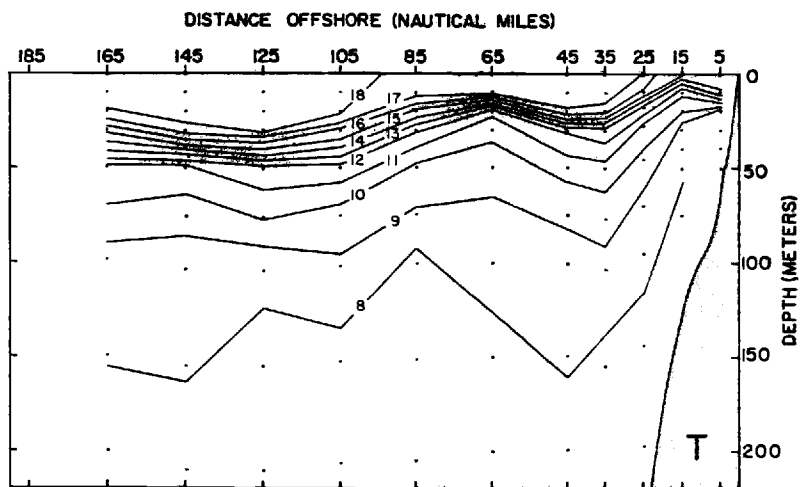
- Reid, J. L., Jr. 1961. On the geostrophic flow at the surface of the Pacific Ocean with respect to the 1,000-decibar surface. *Tellus* 13 (4):489-502.
- Smith, Robert. An investigation of upwelling along the Oregon Coast. Ph. D. thesis. Corvallis, Oregon State University. 83 numb. leaves.
- Smith, R., J. Pattullo and R. Lane. 1966. An investigation of the early stage of upwelling along the Oregon Coast. *Journal of Geophysical Research* 71 (4): 1135-1140.
- Stevenson, Merritt. 1966. Subsurface currents off the Oregon Coast. Ph.D. thesis. Corvallis, Oregon State University. 140 numb. leaves.
- Sverdrup, H. U. 1947. Wind-driven currents in a baroclinic ocean. *Proceedings of the National Academy of Sciences* 33: 318-326.
- Sverdrup, H. U., M. W. Johnson and R. H. Fleming. 1942. The oceans, their physics, chemistry and general biology. New York, Prentice-Hall. 1087p.
- Von Arx, W. S. 1962. An introduction to physical oceanography. Massachusetts, Addison-Wesley Publication Co. 422p.
- Wooster, W. S. and J. L. Reid, Jr. 1963. Eastern boundary currents. In: *The sea*, ed. by M. N. Hill. Vol. 2. New York, Interscience. p. 253-280.
- Wooster, W. S. and B. A. Taft. 1958. On the reliability of field measurements of temperature and salinity in the ocean. *Journal of Marine Research* 17: 552-556.

APPENDIX FIGURES

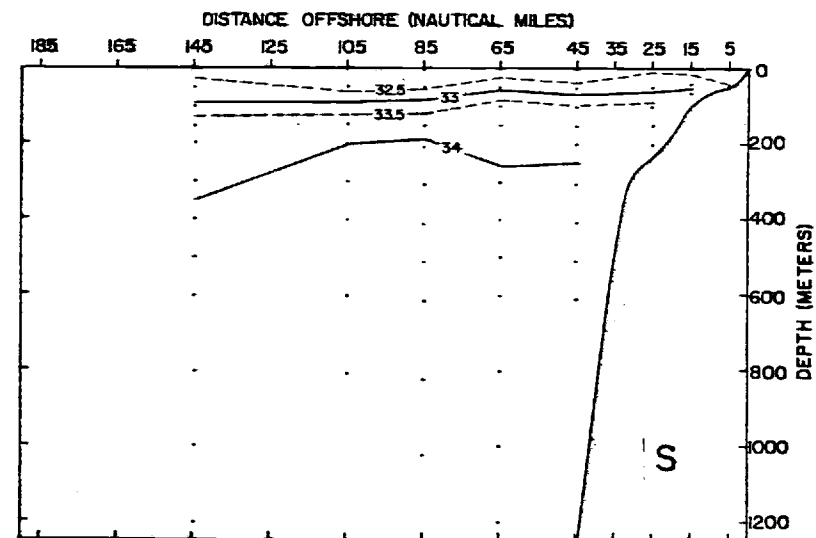
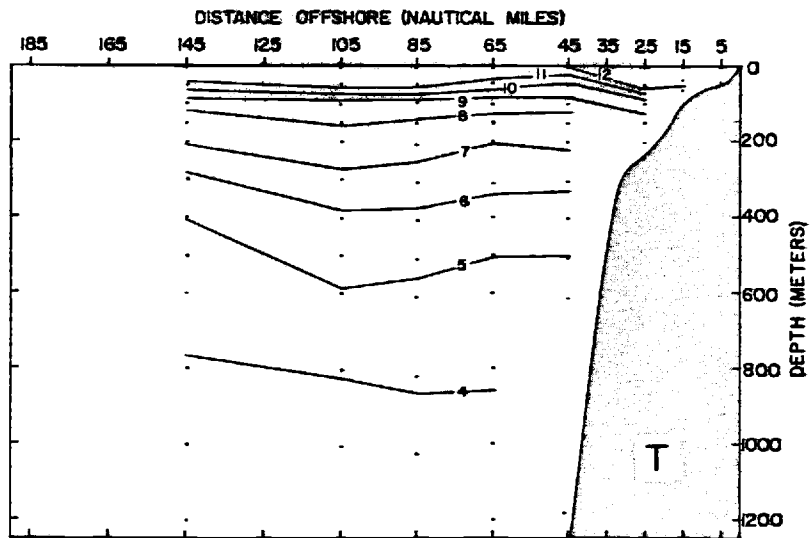
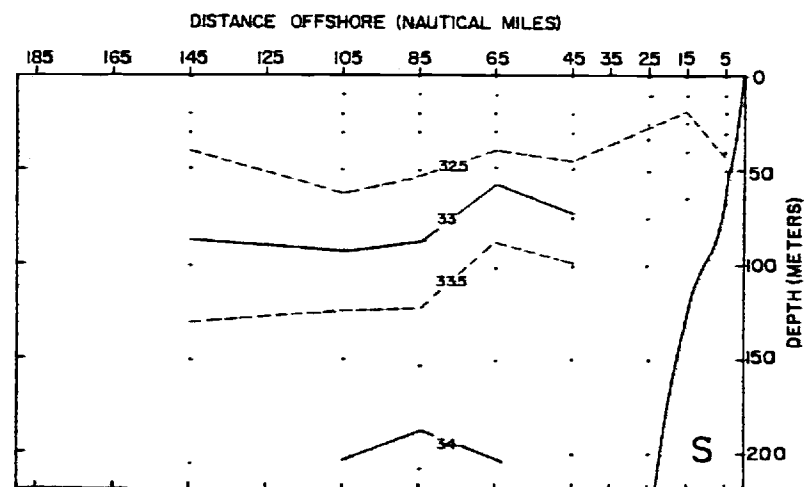
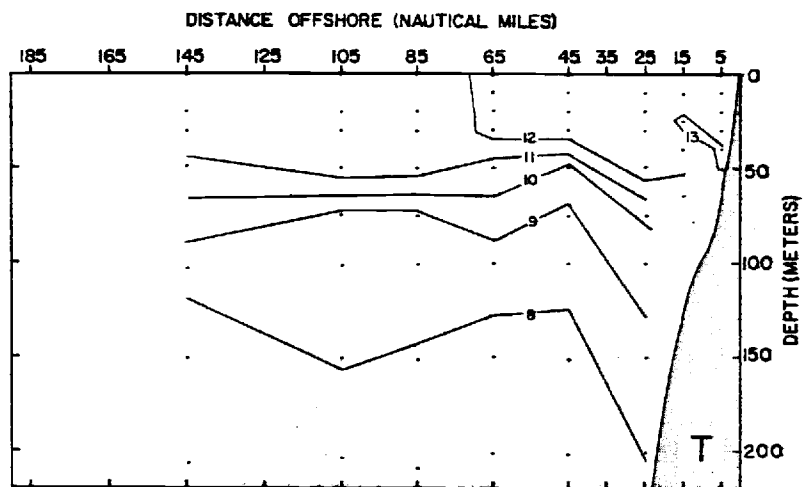
TEMPERATURE AND SALINITY DISTRIBUTION OFF NEWPORT, OREGON



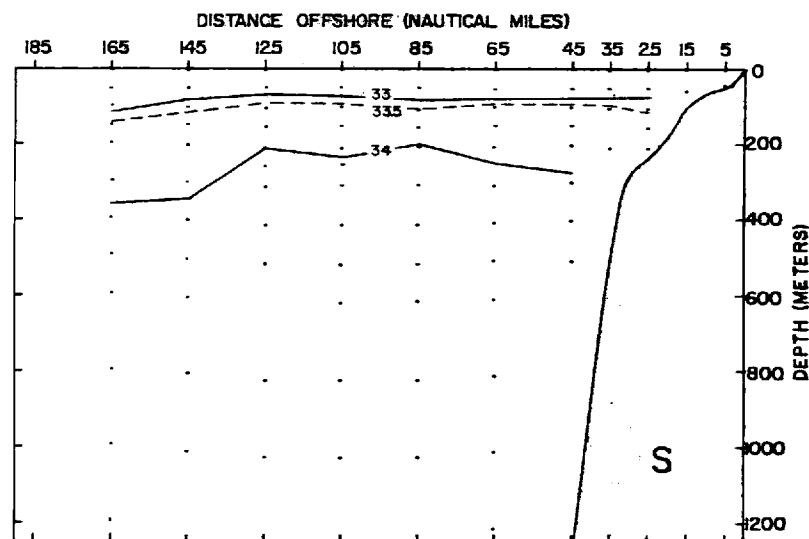
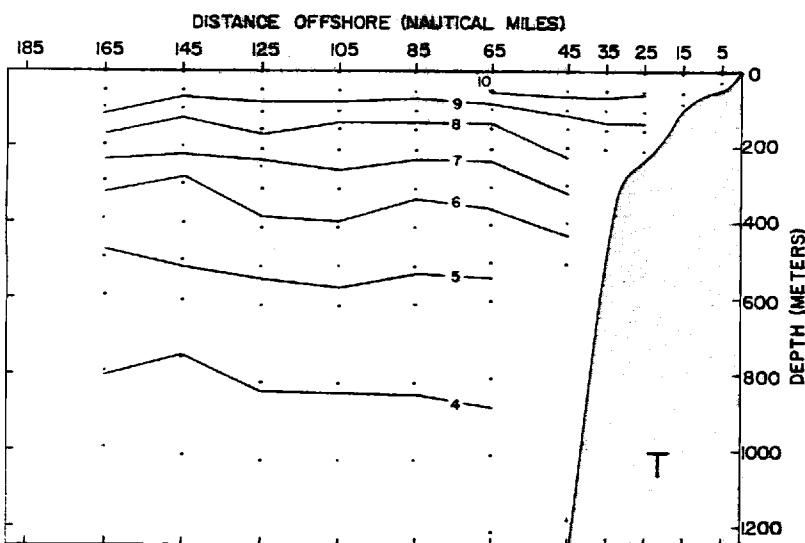
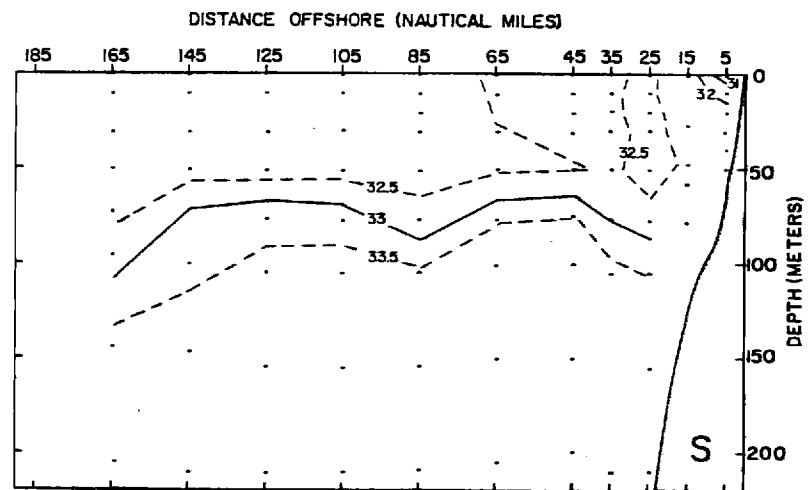
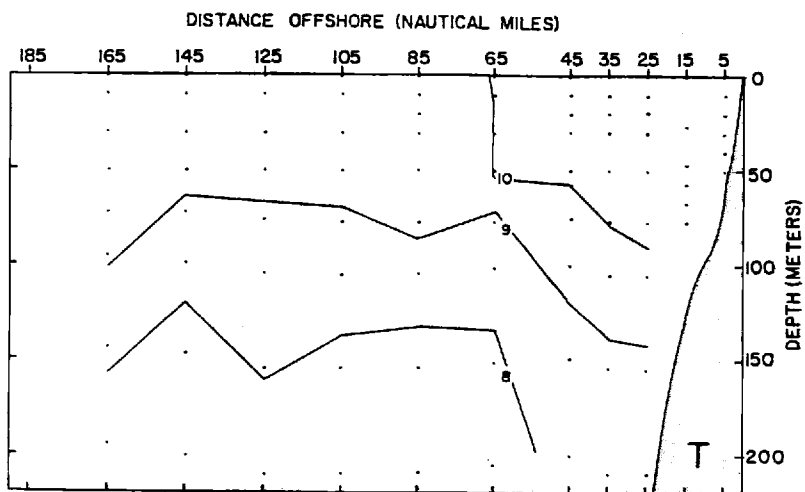
6305 NH



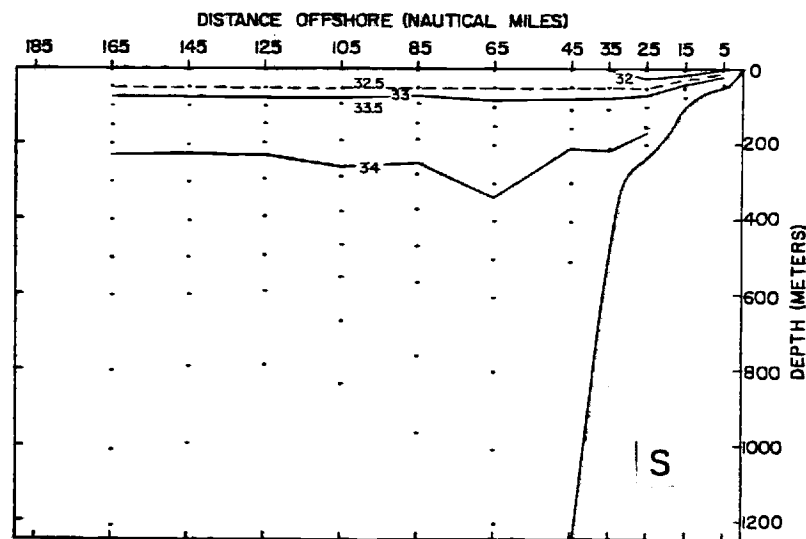
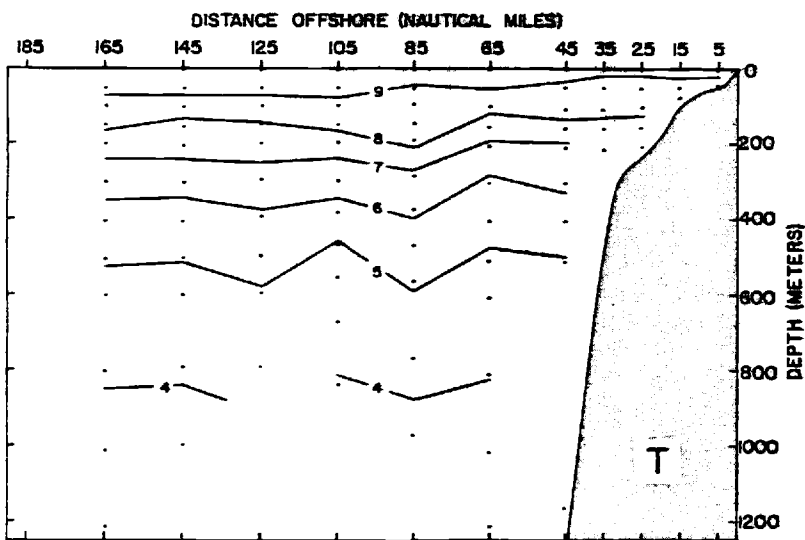
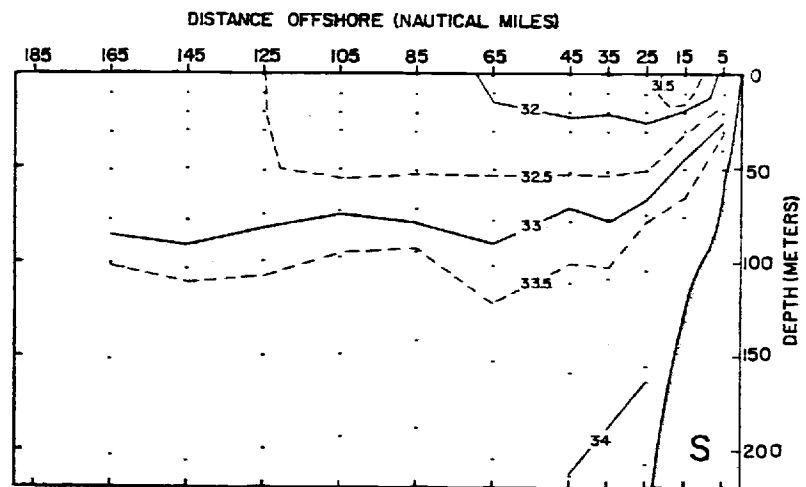
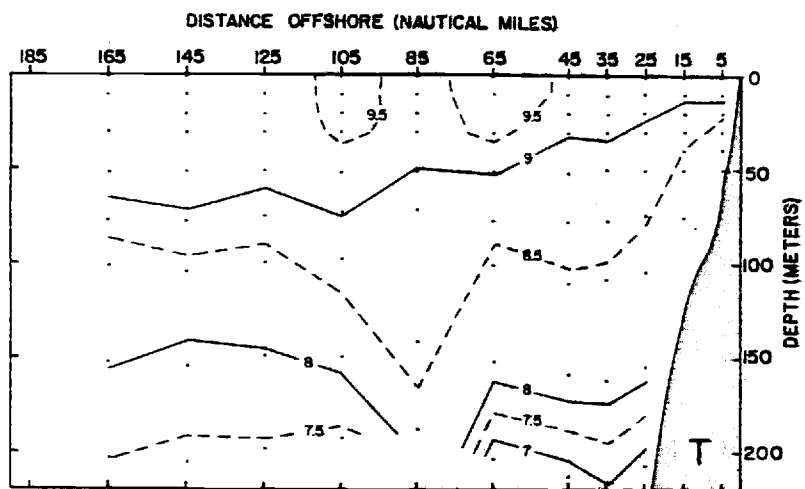
6309 NH



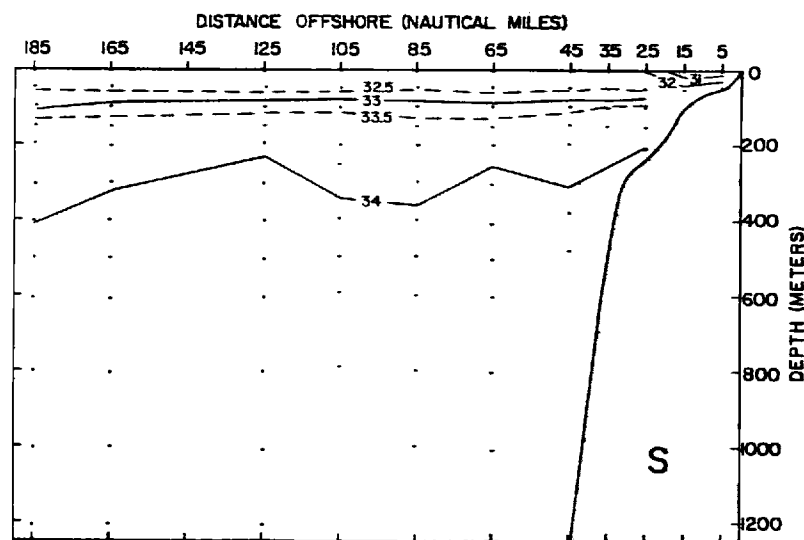
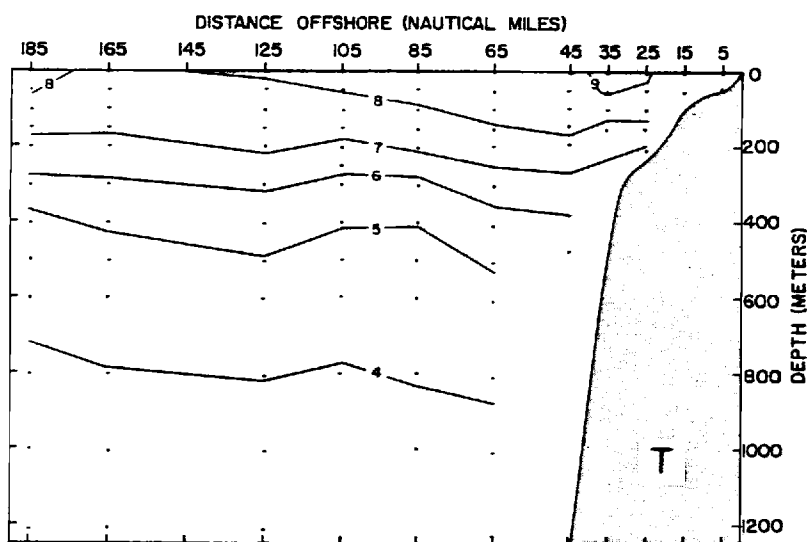
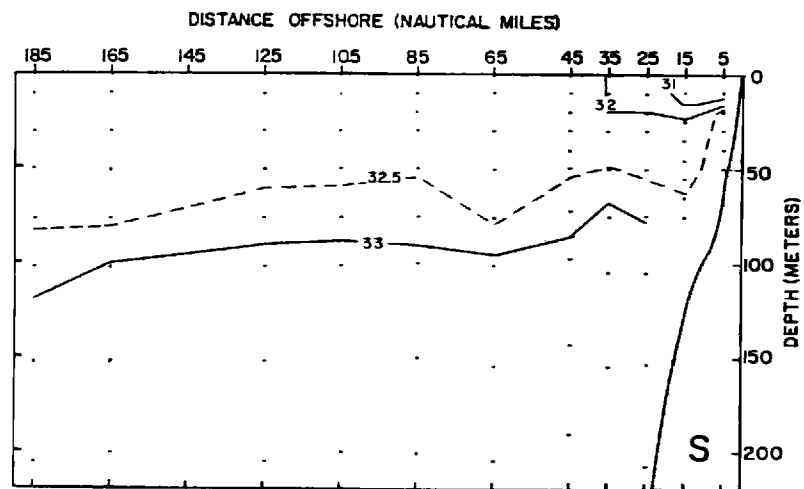
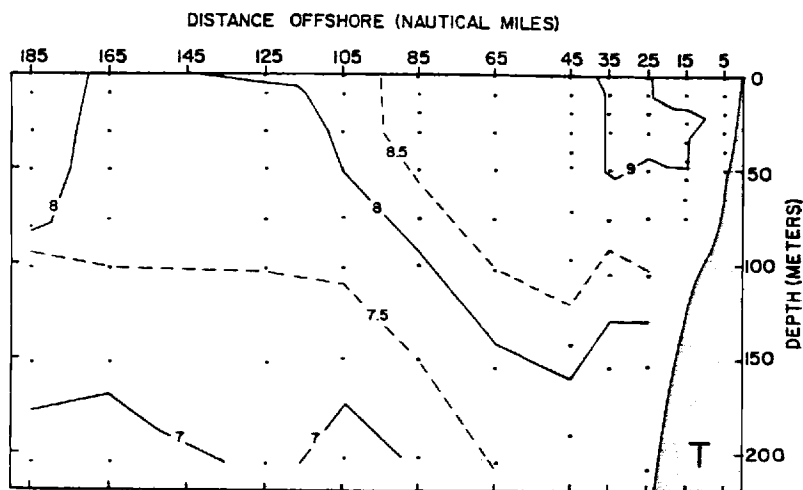
6311 NH



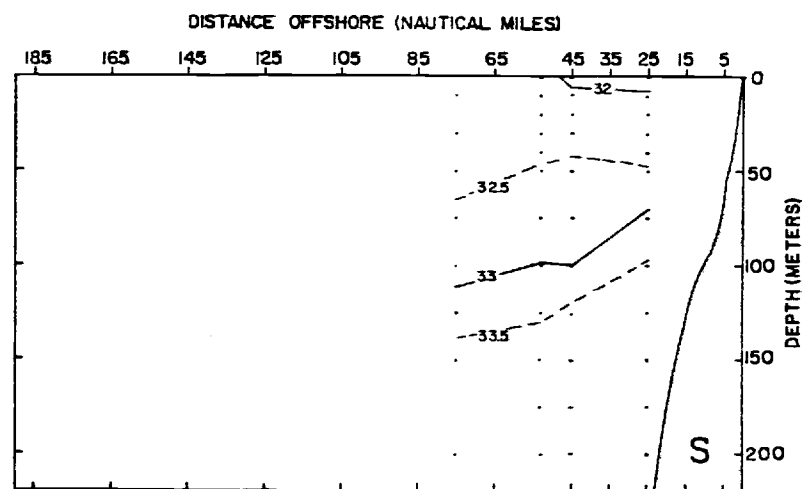
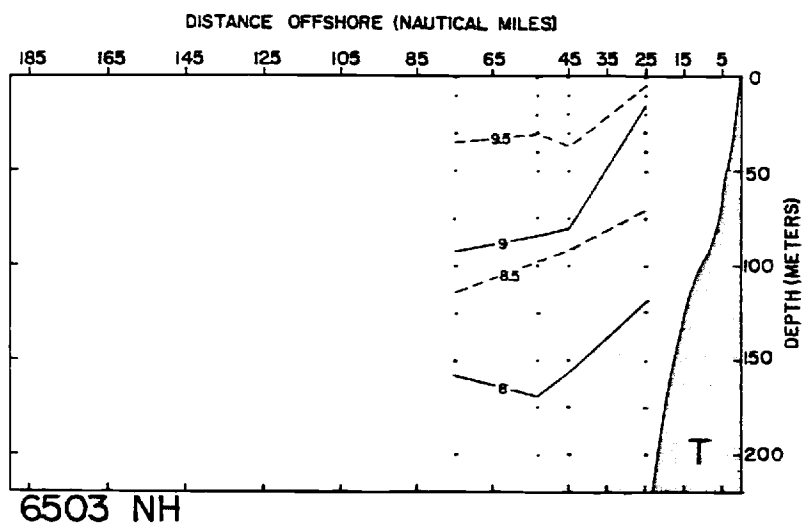
6402 NH

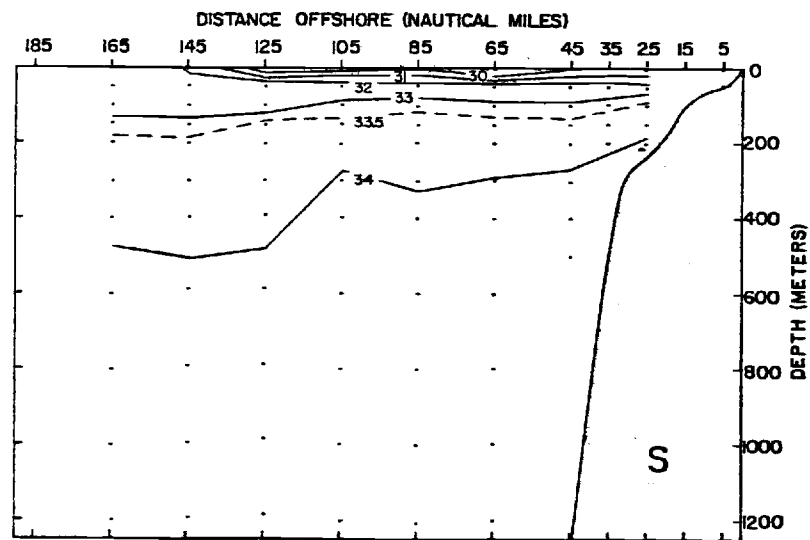
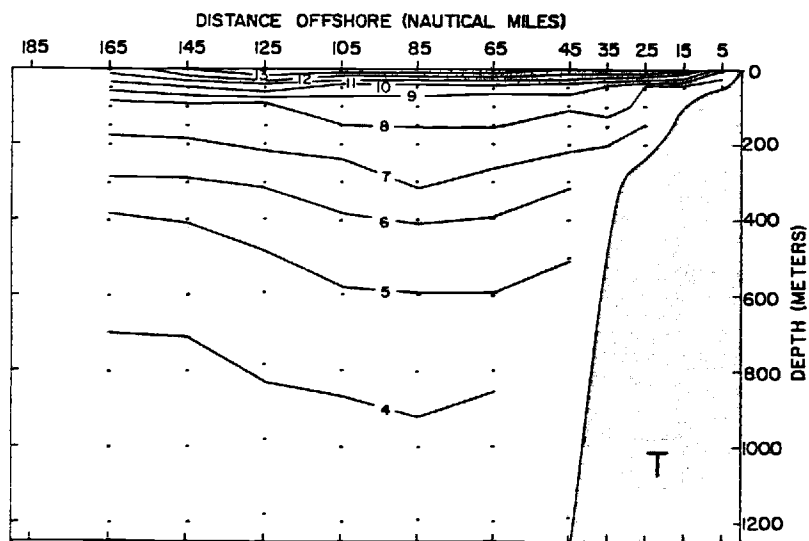
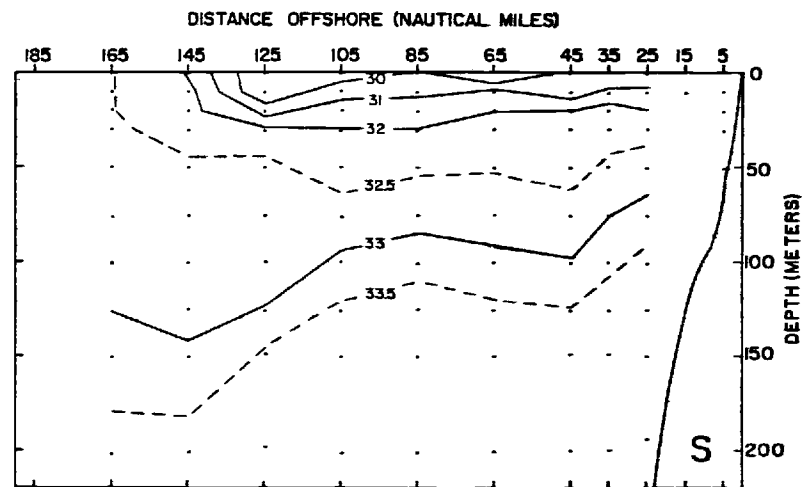
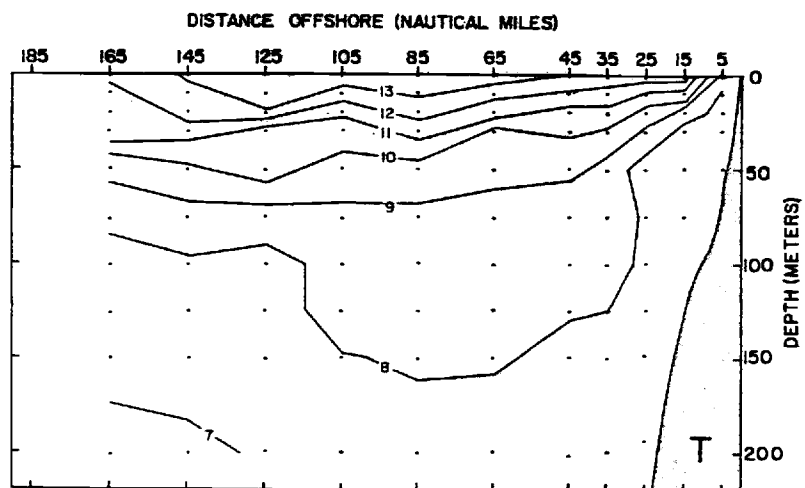


6404 NH

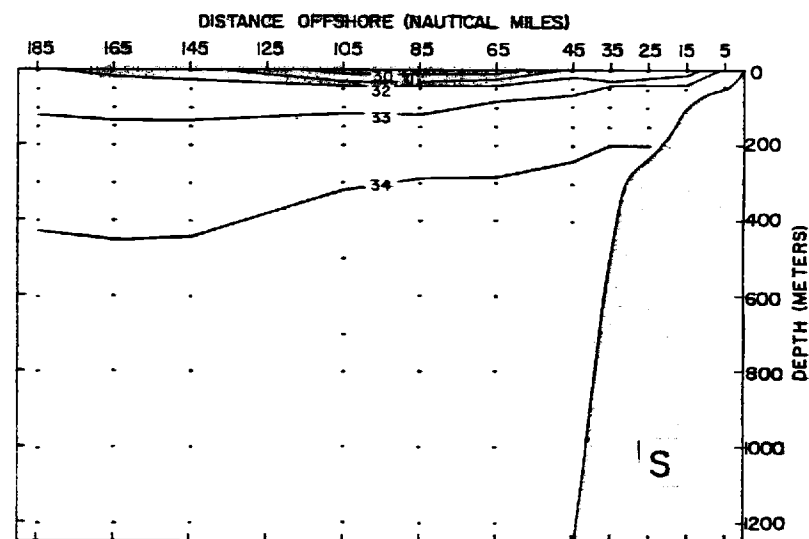
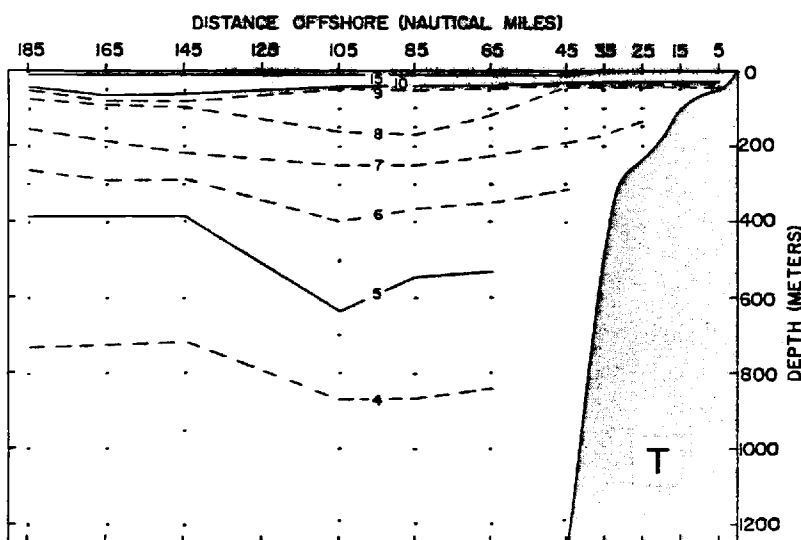
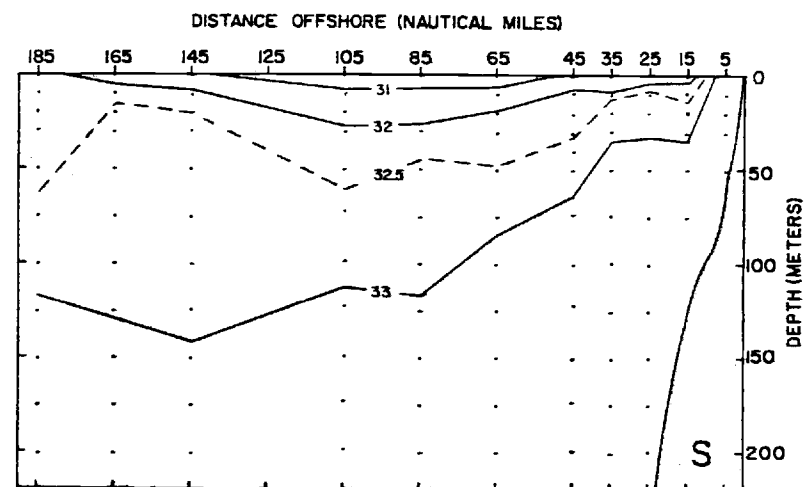
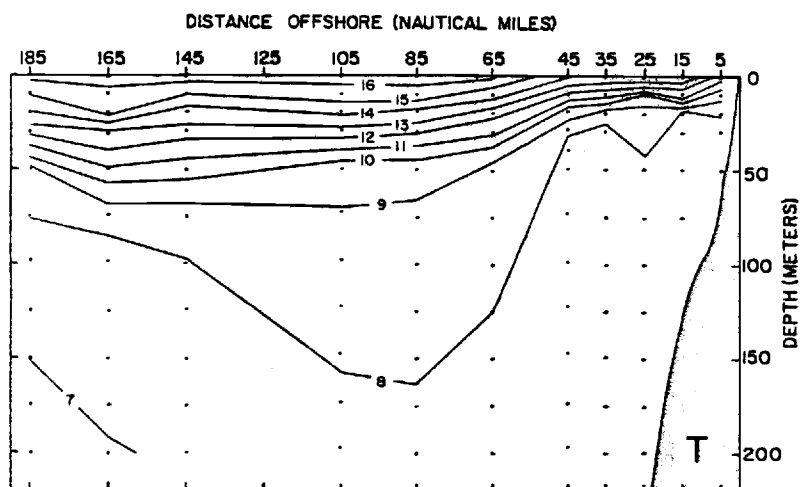


6502 NH

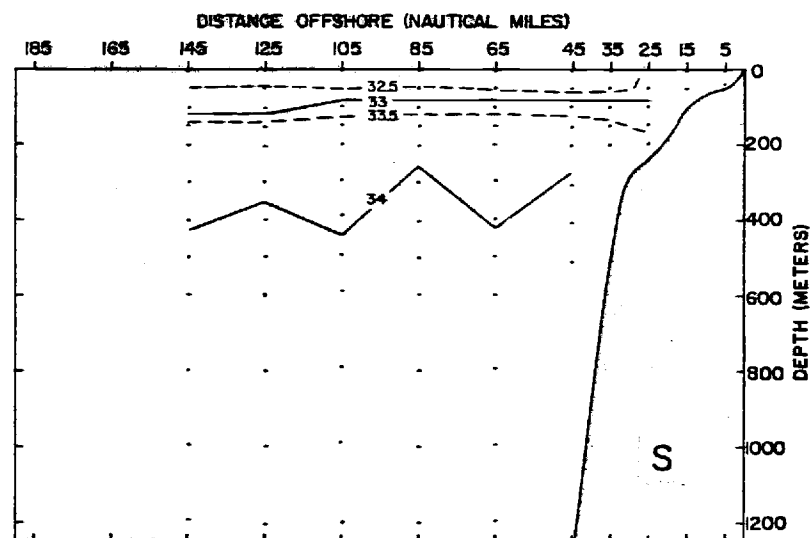
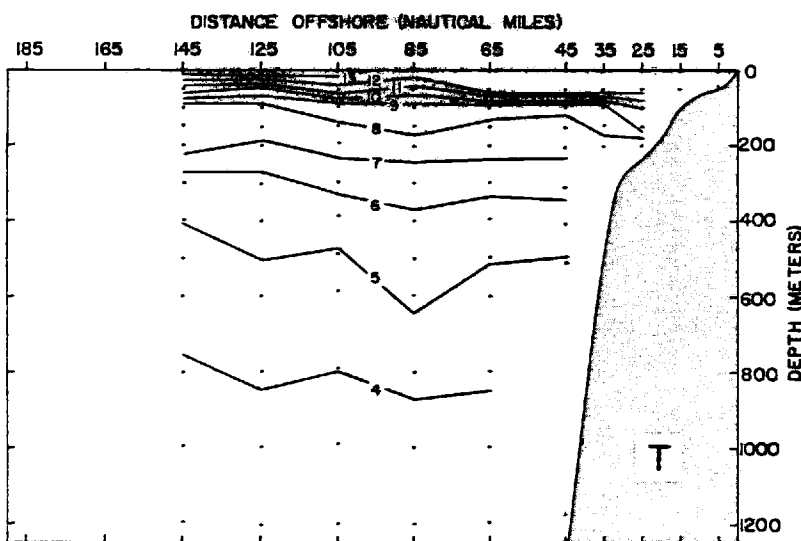
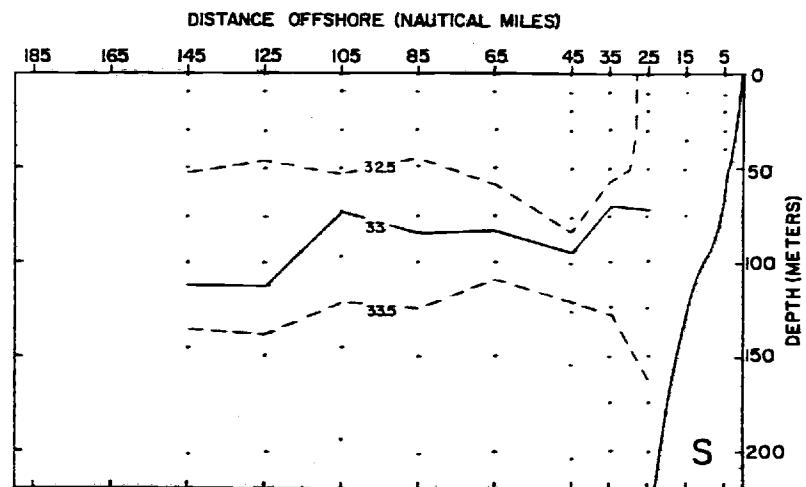
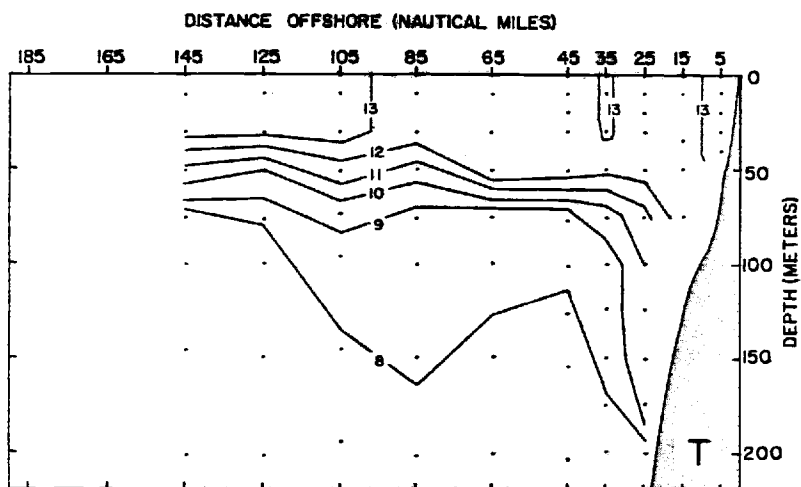




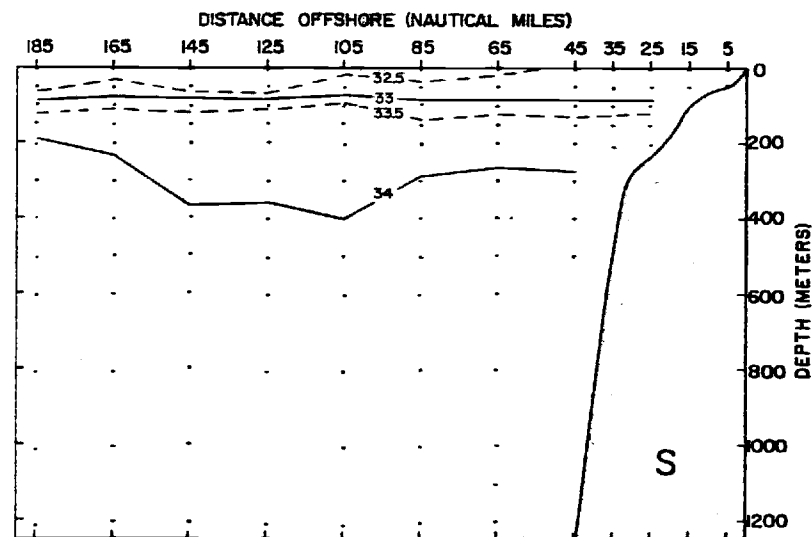
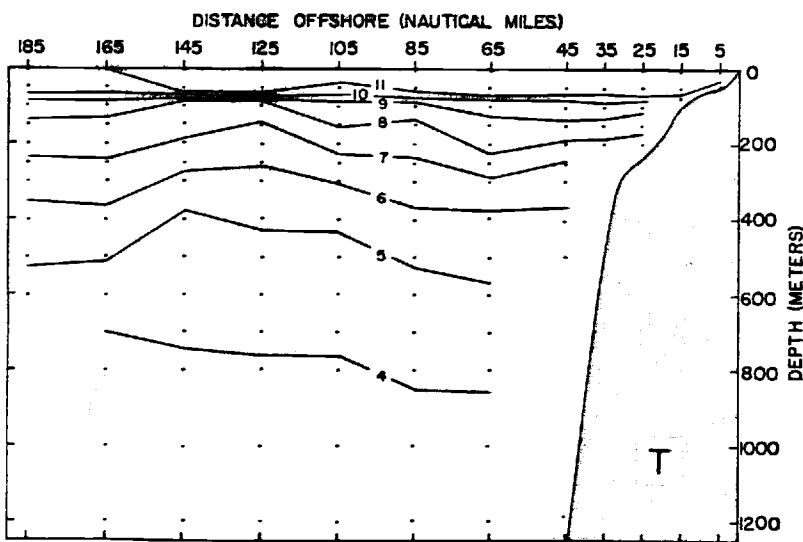
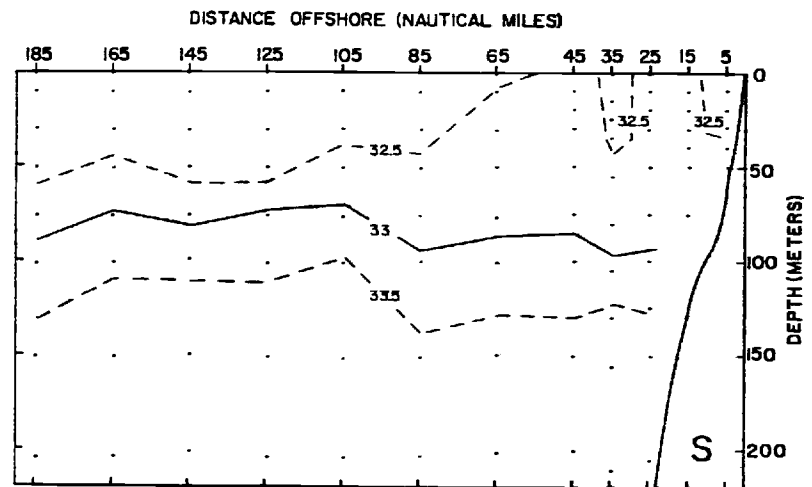
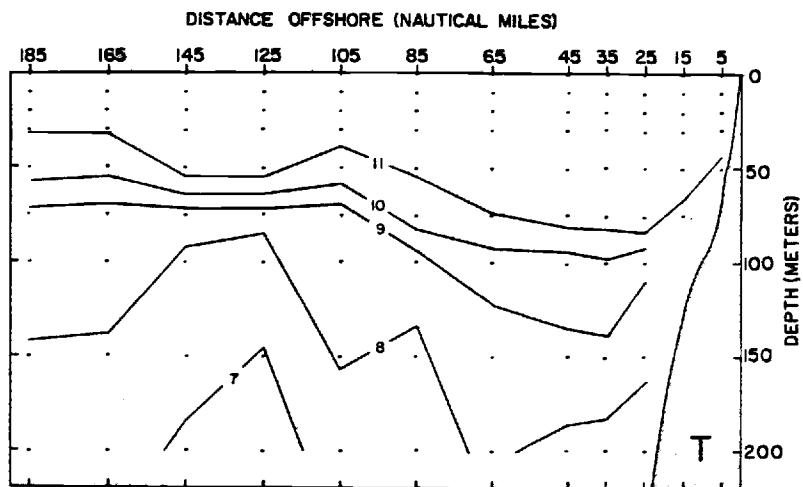
6506 NH



6507 NH



6511 NH



6512 NH